X-ray Photoelectron Spectroscopy

A surface characterization technique

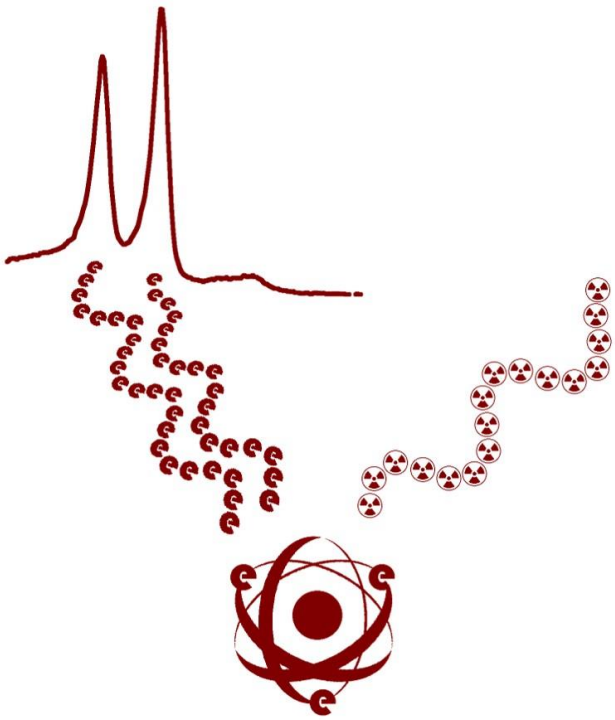

María J. Hortigüela Gallo

Gonzalo Otero Irurueta

universidade de aveiro
theoria poiesis praxis

Título
X-ray Photoelectron Spectroscopy: a Surface Characterization Technique

Autores
María J. Hortigüela Gallo and Gonzalo Otero Irurueta

Editora
UA Editora
Universidade de Aveiro

1ª edição – maio 2019

ISBN
978-972-789-602-8

X-ray Photoelectron Spectroscopy

A surface characterization technique

María J. Hortigüela Gallo

TEMA, University of Aveiro, Portugal

Gonzalo Otero Irurueta

TEMA, University of Aveiro, Portugal

universidade de aveiro
theoria poiesis praxis
dem
department of
mechanical engineering
tema
centre for mechanical
technology and automation

to our families,

Preface

During the last years, an increasing number of students have visited the XPS laboratory for characterizing their samples with this experimental technique. Their background span over a wide range of fields such as physics, material science, chemistry and biology, among others. For most of them, both XPS and ultra-high vacuum technology were something new and they needed help to deal with the data of their samples.

This book tries to concentrate the key information that a young researcher needs for a first approach to XPS. We hope the students will understand its working principle and will obtain the basic tools for analysing their data.

María J. Hortigüela Gallo

Gonzalo Otero Irurueta

May 2019

Acknowledgements

Students, researchers and many colleagues have strongly influenced this book. We would like to thank all of them for their discussions and assistance during the last years at TEMA, University of Aveiro. Moreover, we would also like to thank ESISNA group at Material Science Institute of Madrid for their huge training in Ultra-high Vacuum techniques, including XPS.

This book is supported by the projects UID/EMS/00481/2019-FCT - FCT - Fundação para a Ciencia e a Tecnologia and CENTRO-01-0145-FEDER-022083 - Centro Portugal Regional Operational Programme (Centro2020), under the PORTUGAL 2020 Partnership Agreement, through the European Regional Development Fund

Contents

Chapter 1. Introduction

X-ray photoelectron spectroscopy (XPS) is a surface analytical technique that provides information about the chemistry at the surface of a material. XPS is very versatile and highly sensitive to the last layers of a material, making it quite extended among the several surface characterization techniques. The working methodology is relative simple; a flux of X-ray irradiates a sample provoking the emission of photoelectrons while an electron energy analyser collects them as a function of their energy.

The information that this technique provides is very useful in a wide range of scientific fields. The analysis of XPS spectra allows identifying the elements at a surface and their chemical environment, related to the energy of the emitted photoelectrons. Moreover, the ratio of areas between the XPS peaks is related to the atomic percentage between elements in the sample, so it is possible to obtain an approximation of the stoichiometry of the sample. Almost every element is accessible by XPS with the exception of just Hydrogen and Helium.

No matter the simplicity of the concept, both the experimental set up as well as the interpretation of the data are relative complex. The complexity of XPS systems is largely due to the fact they require ultra-high vacuum conditions (UHV) to work. Thereby, a set of powerful pumps maintain the pressure of the system in the range of 10^{-9} to10^{-10} mbar. Typically, a sample is mounted at the centre of a stainless steel chamber, its surface is irradiated

by the photons and the photoelectrons pass through an electron energy analyser before reaching a detector.

A wide range of samples is accessible by this technique, such as thin films, powders, single crystals, metals, oxides, ceramics, biological samples and composites among others. Even so, there are some limitations mainly related to the stability of the samples at working conditions. The most important limitation is due to the high vacuum environment of the system, excluding the possibility of analysing samples that degas at such a low pressure. The measurement of non-electrically conductive materials is also a delicate issue in XPS, as the emission of photoelectrons induces charges on their surfaces. Nevertheless, the simultaneous injection of a flood of electrons greatly expand the possibilities of analysing insulating materials. Another point to consider is the possible effect of the X-ray beam on the samples. Although XPS uses soft X-ray and in most of the cases is not a destructive technique, X-ray irradiation could cause changes in some sensitive samples. Although historically XPS was mainly associated to surface science groups, nowadays researchers from quite different scientific domains take advantage of this technique. Thus, researchers from Materials Science, Physics, Chemistry, Biology, Geology and others, routinely use XPS as a key experimental technique for sample characterization.

This book resumes the XPS set up in **chapter 2**, the fundamentals of electron spectroscopy in **chapter 3** and describes the standard spectra obtained by XPS in **chapter 4**. Then, **chapter 5** describes XPS depth profile and **chapter 6** shows some practical applications of XPS.

Chapter 2. Experimental set up

This section briefly describes the main parts of the experimental set up required to perform XPS. Figure 1 shows these parts as well as their geometrical configuration. Roughly, it consists in an X-ray source and an electron energy analyzer both focussed on a sample. Moreover, at the end of the analyzer there is a detector of electrons. It measures the quantity of electrons emitted from the sample that reaches the end of the analyzer. Importantly, this set up is inside a vacuum system allowing to the electrons to travel without interacting with anything. Moreover, the main chamber of the vacuum system is shielded against external magnetic fields to avoid or minimize their interaction with the photoelectrons.

The sample is on a 5-axis manipulator allowing choosing the position where do XPS (X, Z axis), the focus or distance between the analyzer and the sample (Y axis) and the polar and azimuthal angles.

Complementary, modern XPS systems use to have a monochromator just after the X-ray source. It is possible to do XPS without a monochromator but their use drastically improve the quality of the spectra.

In the following sections, each of the parts of the system will be described in more depth.

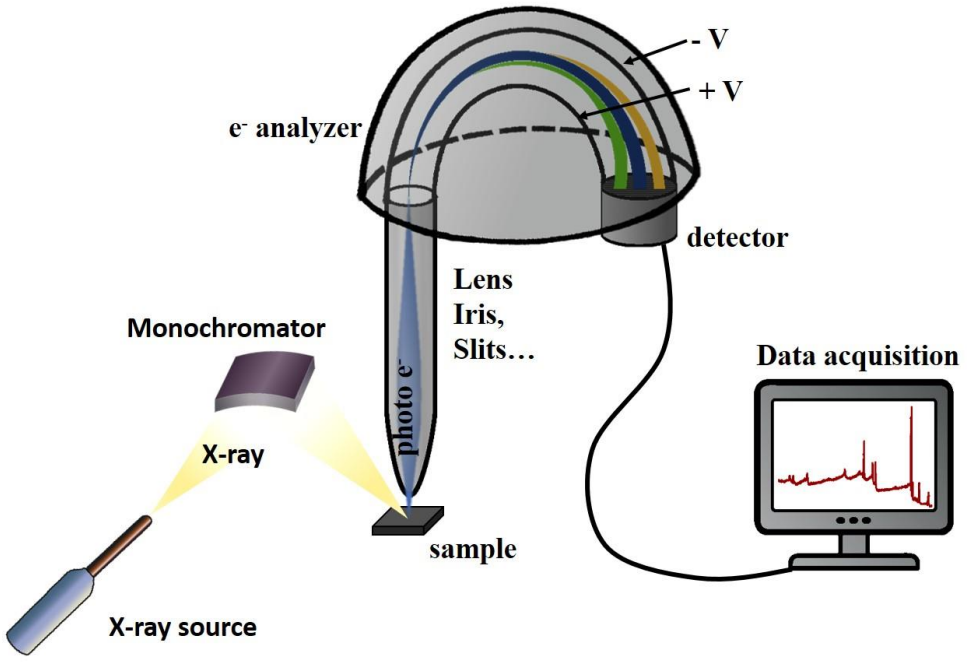

Figure 1. Schematic representation of the XPS experimental set up.

XPS working principle:

- A beam of photons generated by an X-ray source irradiates the sample. The energy of these photons is a known parameter.
- The emitted photoelectrons are guided through the analyzer, which scans in energy.
- The quantity of electrons reaching the detector is counted.
- The output spectra shows counts or number of electrons versus their Kinetic Energy.

2.1. X-ray source

2.1.1. Standard X-ray source

X-ray are generated by irradiating a target material with an energetic electron beam. Thereby, X-ray sources of XPS systems work by bombarding a metallic anode with high-energy electrons. They have three essential components: a pure metal anode, a filament or cathode and a power supply. The cathode emits electrons by flowing an electrical current through it and they are accelerated against the anode by applying a high voltage. Figure 2 shows a schematic representation of a laboratory X-ray source.

The energy of the X-ray is characteristic of the anode material, while the intensity of the beam depends, among others, on the amount of electrons bombarding the anode. Thus, it can be regulated by adjusting the electrical current trough the cathode. Mg and Al are the most used materials for doing anodes. They produce Mg Kα and Al Kα radiation with energies of 1253.6 eV and 1486.6 eV, respectively.

The energy of the photons depends on the material of the anode

Furthermore. Since during X-ray generation most of the energy of the projectile electrons is transformed in heat, it makes necessary a water cooling system that refrigerates the anode to avoid the overheating of the system.

Nowadays, it is usual to combine the above described X-ray source with a monochromator (quartz single crystal). It rejects the X-ray of undesired energies such as minor X-ray lines and white radiation, and focus the filtered beam into the sample. This monochromatic X-ray beam, narrower in photon energies, produces XPS spectra with higher resolution and

minimizes the probability of damaging the sample. We remark that it is not necessary to use a monochromator to perform XPS but its use improves the quality of the final spectra.

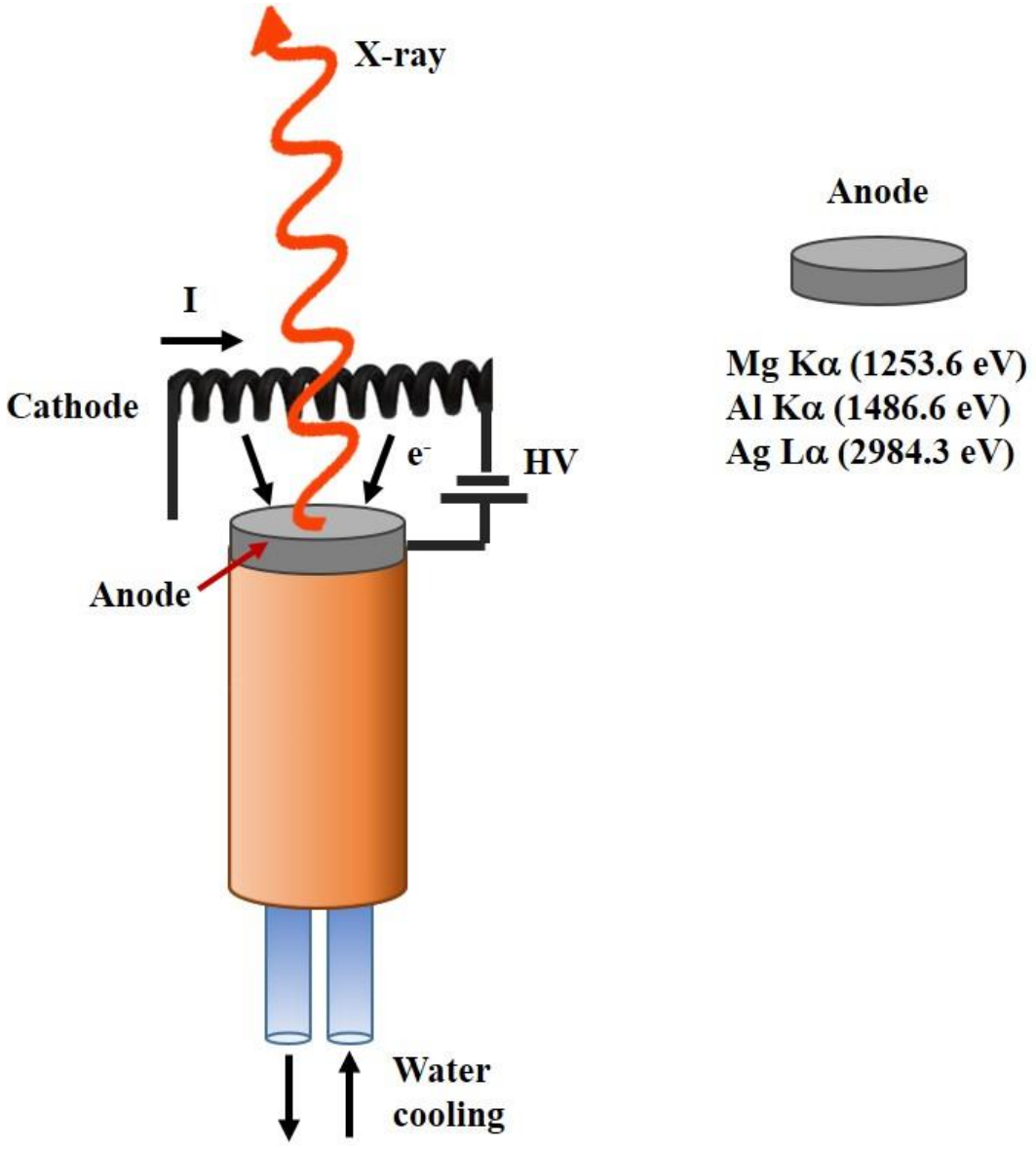

Figure 2. Schematic representation of an X-ray source used in a XPS laboratory.

2.1.2. Synchrotron radiation facility

Synchrotron radiation is generated when electrons traveling with enough energy change their direction. A synchrotron radiation facility consists in a storage ring where electrons are forced to circulate at high speed and turn by applying magnetic fields to some specific positions of the ring. The electromagnetic radiation generated this way cover a broad range of frequencies, including X-ray.

The electrons for the storage ring are generated by an electron gun, which is typically a Linac. This first stage generates and accelerates the electrons for their injection in a Booster, which accelerates the electrons at higher energies. Then, after passing the Booster, the electrons are finally injected in the storage ring.

These large facilities allow the selection of light with a suitable wavelength for a variety of experimental techniques. Thereby, X-ray can be collected and directed to a vacuum chamber to do XPS.

The X-ray radiation obtained in a synchrotron has several advantages with respect to that obtained by a standard X-ray source. On one hand, the X-ray beam is much more intense, strongly diminishing the time needed to measure a sample by XPS. On the other, the energy of the photons can be fine-tuned allowing doing XPS with X-ray of different energies. Moreover, the X-ray are truly monochromatic, improving the resolution of the XPS spectra.

In a synchrotron:

- Variable photon energy
- Very high intensity
- High resolution XPS

2.2. Electron energy analyzer

As it was previously mentioned, the irradiation of a sample by X-ray produce the emission of photoelectrons. A spectrometer or electron energy analyzer works by filtering the photoelectrons as a function of their kinetic energy. Figure 3 shows a representative image of a hemispherical electron energy analyzer, the most used spectrometer nowadays.

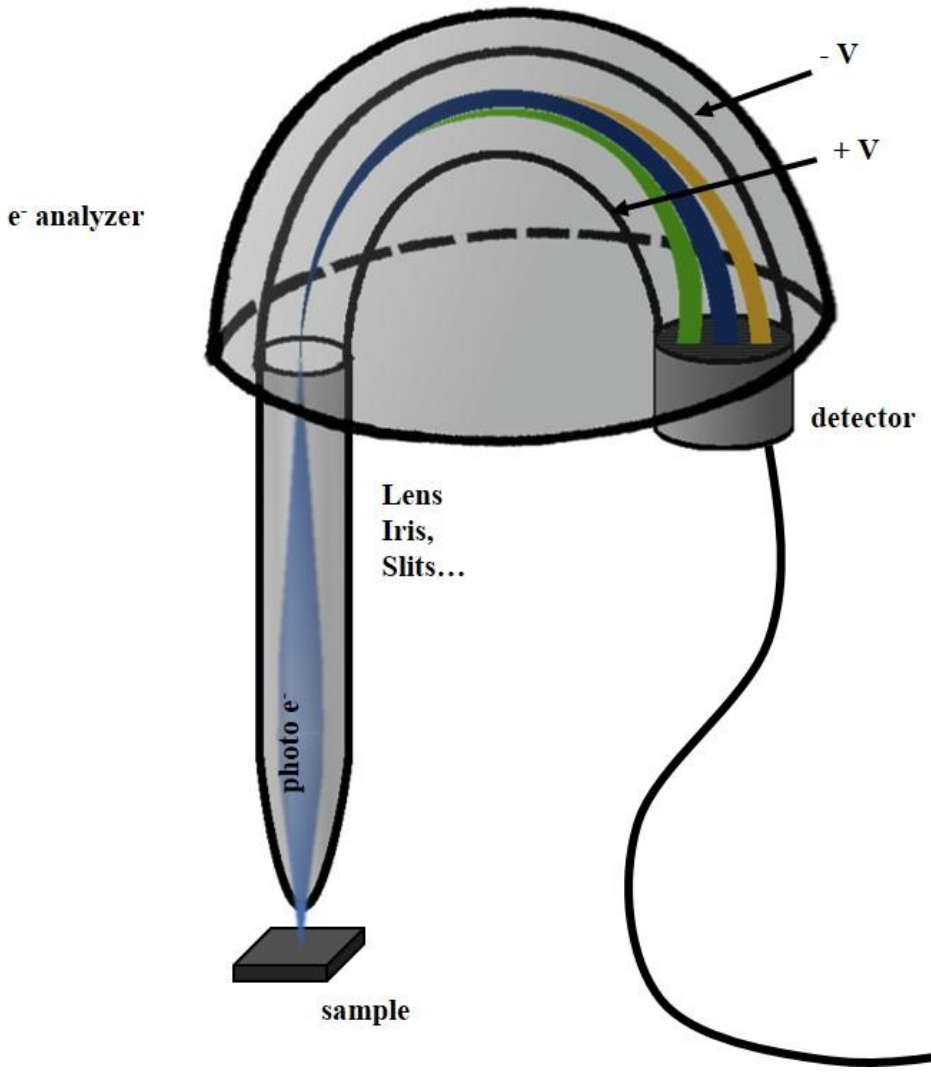

Figure 3. Schematic representation of a hemispherical electron energy analyzer.

The analyzer consists of two parts: a first column near the sample followed by a hemisphere.

Inside the column, an electrostatic lenses system (transfer lenses) slow down the photoelectrons to a preselected value (pass energy) and focus them into the entrance of the hemispherical part. By modifying the voltage applied to these lenses, they can slow down photoelectrons with different kinetic energies.

The hemisphere is an electrostatic analyzer that disperses the electrons as a function of their energy. Inside it, there are two hemispheres of different radii connected to different voltages. These voltages determine the pass energy of the analyzer, parameter involved in the resolution of the spectra.

Thus, photoelectrons with an energy slightly higher or lower than the preselected pass energy, reach the detector at different points (yellow and green pathways in figure 3). Hence, photoelectrons with an energy significantly higher or lower than the preselected are diverted and will not reach the detector.

The spectrometer allows the photoelectrons with a desired energy to reach the detector

XPS energy analyzers can work under different modes; nevertheless, the most usual operation mode is the so-called fixed analyzer transmission (FAT). In this mode, the pass energy is held constant during the measurements while the electrostatic lens inside the column scans in energy. In FAT mode, since the pass energy does not change trough the spectra, the resolution of the XPS peaks is the same independently of their energy.

In FAT mode, the resolution of XPS peaks with different energy is the same

2.3. Detector

Once the photoelectrons with the preselected energy reach the end of the spectrometer, they reach a detector. Its mission is essentially to count electrons per unit of time. Figure 4a shows a photo of a detector of electrons while its working mode is represented in figure 4b.

The detector works basically as an electron multiplier. When an electron crashes at the entrance, several secondary electrons are generated inside the detector. Then, the secondary electrons crash again inside the detector producing more and more electrons. The resultant avalanche of electrons is guided towards the exit by applying a high voltage. Finally, an electronic circuit measures the electrical current at the exit of the detector. The measurement software transform the information into spectra showing the number of electrons versus the energy.

A detector is an electron multiplier.

It counts the quantity of electrons during a selected time

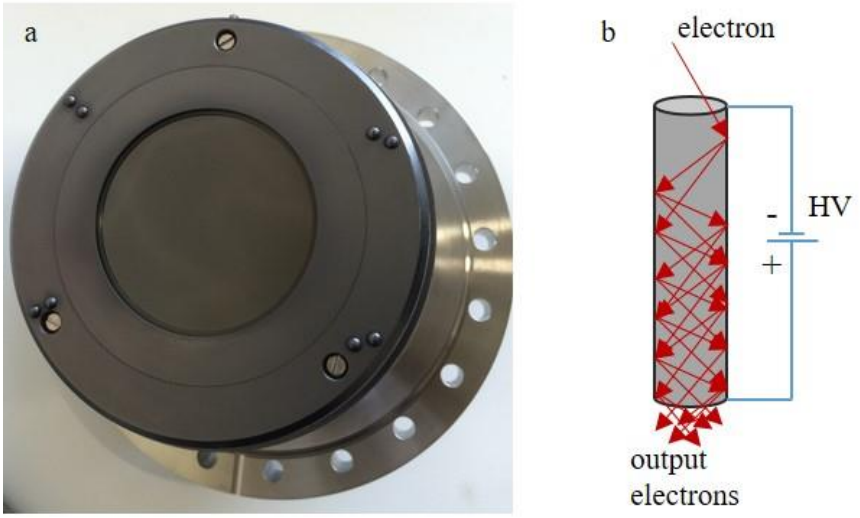

Figure 4. a) Photo of a detector. b) Schematic representation of the working principle.

2.4. Vacuum system

An XPS system works under high vacuum or ultra-high vacuum (UHV) conditions due to several reasons. The first one is that the photoelectrons, after leaving a sample, have to travel large distances without interacting with anything. A second key reason is to avoid atmospheric contamination at the surface of the sample during the experiments.

Typically, an ultra-high vacuum system has several vacuum pumps working at different pressures. They are schematically represented in figure 5.

- Rotatory pumps / scroll pumps: from atmospheric pressure to 10^{-2} mbar.
- Turbomolecular pump: from 10^{-2} mbar to 10^{-9} mbar.
- Ion pump: from 10^{-8} mbar to 10^{-11} mbar.
- Titanium sublimation pump (TSP): from 10^{-9} mbar to 10^{-11} mbar.

A rotatory pump as well as a scroll pump are rough compressors of air. Nowadays, a scroll pumps are preferred instead of the old rotatory pumps because they do not use oil. The oil of the rotatories can slowly go inside the XPS system contaminating the UHV chamber.

A turbomolecular pump works as a turbine, by giving momentum to the molecules that are inside the chamber. At its exit, a scroll pump is connected in series for exhausting the gas.

In parallel to the turbomolecular pump, the vacuum chamber has an ion pump and a TSP. The ion pump consists in a set of parallel electrodes connected to a high voltage difference. It works by ionizing the gas,

accelerating these ions by the high voltage and finally trapping them into the solid electrode. These three type of pumps are active components working continuously. On the other hand, a TSP works by periodically sublimating titanium from a filament to the surrounding walls of the vacuum chamber. Since clean titanium is a quite reactive material, the residual gas molecules bond to it once randomly encounter it. For avoiding the deposition of titanium on the key parts of the system, the TSP is in a small container at a corner of the system.

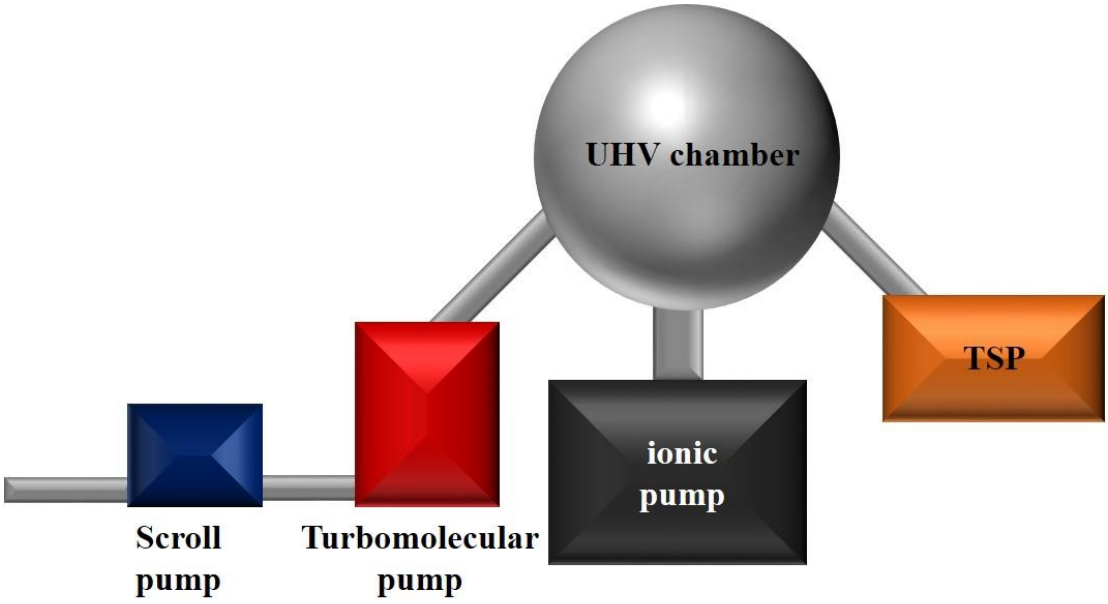

Figure 5. Schematic representation of the UHV pump system.

The vacuum pumps maintain a pressure in the range of 10^{-10} mbar during the experiments. At this pressure:

- Electrons can travel a large distance without energy loss
- The surface under study is not contaminated during the experiments

2.5. Bake-out of an Ultra-High Vacuum system

Even by having a set of very powerful vacuum pumps, it is not easy to reach UHV conditions. From atmospheric pressure, the system needs to be baked-out during around two days to reach 10^{-10} mbar. The whole system, after removing plastic parts, is enclosed into an aluminium box and warmed up by using external heaters. The typical procedure is to heat up at 100 – 120 °C during one or two days. The contamination deposited on the internal walls and components, mainly water, is slowly detached and pushed out by the vacuum pumps. There are some requisites to consider during this process:

1. The temperature should be homogeneous through the while system.

2. The temperature should be slowly increased. Typically, it takes 4-6 hours for going from room temperature to the target temperature.

3. After two days, the temperature should be slowly decreased.

4. Special attention should be taken in key parts of the system, as it could be windows, XPS detector and monochromator.

Moreover, to get the system ready to work, every active component of the system should be slowly degassed after the bake-out. That includes any filament, X-ray source, XPS detector and so on.

Each time the vacuum pumps have to be stopped for any reparation inside the chamber, the whole process to recover the UHV takes around three or four days, depending on the system. That is the reason to emphasize the importance of a careful maintenance to keep an UHV system under working conditions daily.

Working conditions are reached after:

- Two days of bake-out
- Degassing any internal component

Chapter 3. Electron spectroscopy

Electron spectroscopies, as general concept, analyse the electrons emitted when a sample is irradiated. When using photons to pull out the electrons, then it is named photoelectron spectroscopy (PS). According to the energy of the photons, UV light is able to eject valence electrons (UPS) while X-ray, with higher energy, release also electrons from core level orbitals (XPS).

The energy needed to eject an electron, depends on the electronic structure of the chemical species. From the theoretical point of view, Koopmans's theorem identify the ionization energy with the negative of the energy of the orbital, when considering equals the orbitals before and after ionization. When assuming relaxation by electronic rearrangement, then the variation of energy is the difference between energies of initial and final state, *i.e.* neutral molecule and ion.

In the case of atoms (figure 6a), whose electrons are at different three-dimensional atomic orbitals, the set of energies of these orbitals is different for each element. It depends on the electrostatic interactions with the nucleus and the shielding from the rest of electrons. Thus, by measuring the energy of the electronic levels it is possible to identify the element.

When atoms bond in molecules, atomic orbitals combine in molecular orbitals. Although only the outermost electrons participates in chemical bonding, inner electronic orbitals are also affected. The redistribution of

the electronic charge due to the chemical bonding alters the electronic shielding and thus the energy of the inner orbitals.

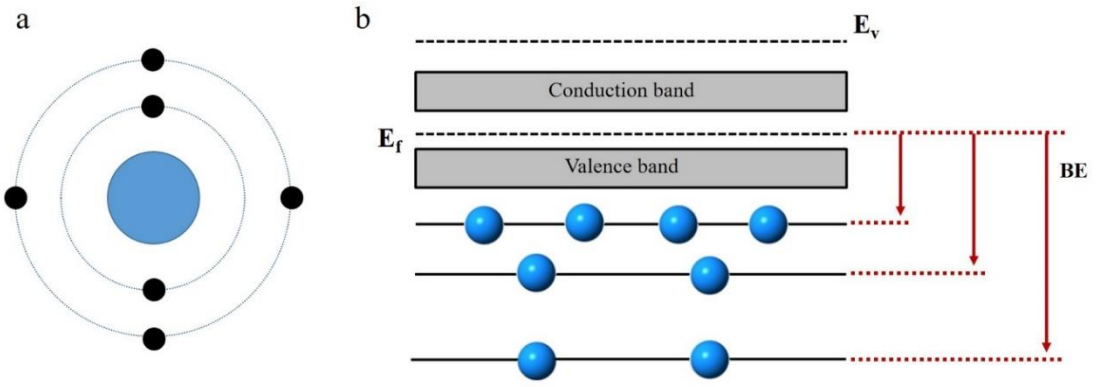

Figure 6 shows simplified diagrams of the electronic structures of an arbitrary element (a) and a solid (b).

In the case of a solid, the atomic discrete levels of energy become bands due to the huge amount of atoms involved. Core levels form narrow bands while shell orbitals leads the formation of the wider valence and conduction bands (figure 6b).

The fact that inner orbitals partially retain their atomic character, allows the elemental identification by measuring their energy. At the same time, the slight change of energy of core electronic levels due to the chemical bonding reveals information about the oxidation state and the local chemical environment of an element in a chemical specie.

By measuring the energy of the electronic levels, it is possible to identify the elements at the surface of a sample as well as their chemical environment

3.1. X-ray photoelectron spectroscopy (XPS)

XPS measures the number and kinetic energy of electrons ejected from a sample because of the incidence of X-ray photons. The main photoemission process in XPS is the ejection of core level electrons through a transfer energy process from the photons. Figure 7 schematically shows this phenomenon. A photon irradiates the sample and transfers its energy to an electron that leaves the sample.

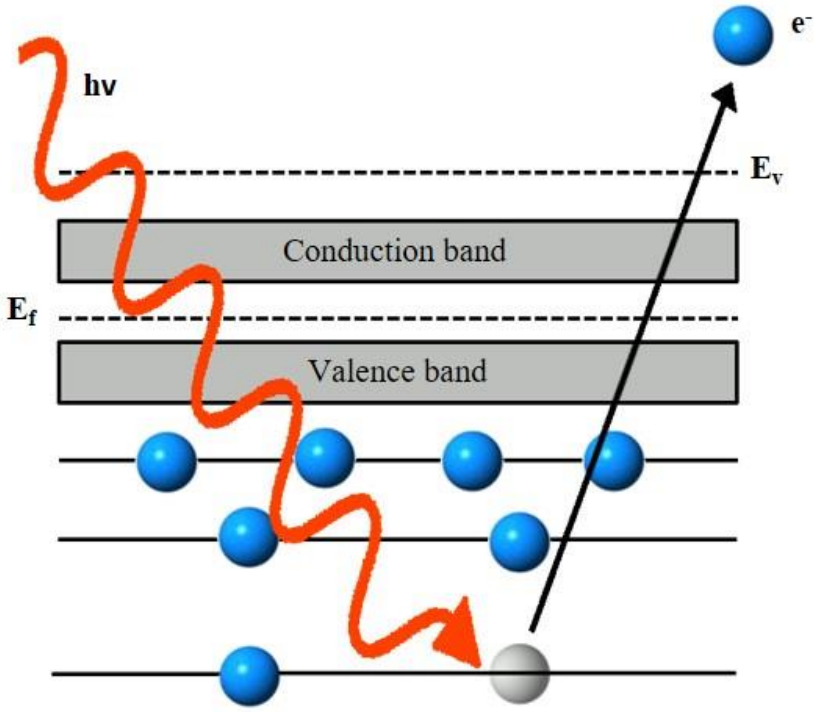

Figure 7. Schematic representation of the XPS process. On the left, photons with hν energy irradiate the sample and transfer its energy to core electrons. On the right, the photoelectrons leave the sample with the energy obtained from the photons.

This is an elastic process *i.e.* photons completely transfer their energy to electrons. When the electrons leave the sample without interacting with anything else and reach the spectrometer, the relationship between the measured kinetic energy, the binding energy and the energy of the photons is given by equation 1.

$$BE = h\nu - KE - \phi_s \qquad \text{Eq. 1}$$

In which BE is the binding energy, hν is the energy of the photons produced by the X-ray source, KE is the kinetic energy of the photoelectrons measured by the spectrometer and ϕ_s is the work function of the spectrometer.

XPS is an elastic process:

$BE = h\nu - KE - \phi_s$

We notice that only the core levels with a BE lower than the energy of the photons are accessible by XPS. It is also important to emphasize that this is a surface characterization technique, since the possibilities that an electron leave the sample without suffering any interaction drastically decreases with the depth.

3.2. XPS notation

This section shows the relationship between the quantum numbers and the XPS notation. Table 1 summarizes this information.

Quantum numbers				XPS notation
n	l	s	J	
1	0	+1/2; -1/2	1/2	1 s
2	0	+1/2; -1/2	1/2	2 s
2	1	-1/2	1/2	2 $p_{1/2}$
2	1	+1/2	3/2	2 $p_{3/2}$
3	0	+1/2; -1/2	1/2	3 s
3	1	-1/2	1/2	3 $p_{1/2}$
3	1	+1/2	3/2	3 $p_{3/2}$
3	2	-1/2	3/2	3 $d_{3/2}$
3	2	+1/2	5/2	3 $d_{5/2}$

Table 1. Relationship between the quantum numbers and XPS notation

Core levels in XPS use the nomenclature nl_j, where n is the principal quantum number, l the azimuthal quantum number, s the spin and j is the total angular momentum (j = l + s).

The spin-orbit interaction give rise to two possible energy states for each level, excepting s levels, e.g. Cu $2p_{1/2}$ and Cu $2p_{3/2}$. This phenomenon is known as spin-orbit splitting. There are a couple of considerations about it to take into account when interpreting XPS spectra. On one hand, the possibilities to find an electron in each state of these couples depends on their degeneration (2j + 1). Thereby, it is known the relative ratio of electrons emitted from these pairings, so the relative areas of their XPS peaks: approximately 1:2, 2:3 and 3:4 for p, d and f orbitals, respectively. On the other hand, the difference of binding energy between both peaks of each couple for each element is very similar in different chemical compounds, and these data can be found in XPS databases.

3.3. Auger electron spectroscopy (AES)

It was previously mentioned that XPS is the main emission process when irradiating a material with X-ray, but it is not the only one. After the emission of an electron induced by photons (figure 8a), the atom is excited and has to relax. There are several relaxation processes but an Auger process is one of the most probable. In this process, an electron from a higher level decays to fill the hole in a deeper level (figure 8b) and the energy released from this decay is transferred to another electron, allowing its scape from the sample (figure 8b). This last electron is the so-called Auger electron.

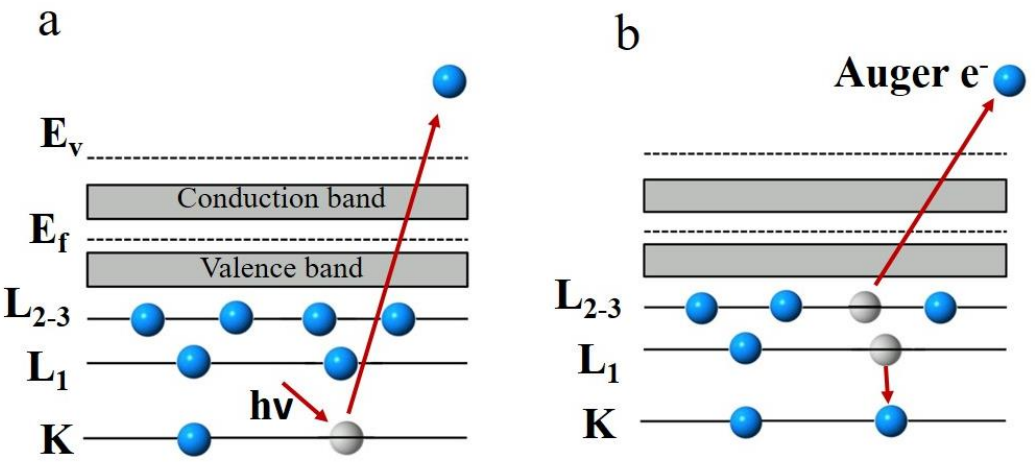

Figure 8. Auger relaxation process. a) Ionization of the atom. b) decay of an electron from a higher level and scape of another electron (Auger electron) from the sample.

Kinetic energy of Auger electrons do not depend on the energy of the photons but on the energy of the electronic orbitals involved in the process. Since orbitals energy are

Auger electron spectroscopy:

Elemental composition and their chemical environment

characteristic of the element and its interaction with other atoms, Auger electrons also render information to identify the elements at the surface of a sample and their chemical environment.

It is also worth mentioning that although X-ray induced Auger emission is a natural and inevitable process taking place during XPS, AES is an independent technique, most commonly using an electron gun to produce the initial electronic emission.

Auger notation consist in the element followed by the three levels involved in the Auger process, e.g. C KLL.

3.4. Ultra-Violet photoelectron spectroscopy (UPS)

During XPS experiments, it is also possible to pull out valence band (VB) electrons besides deeper core level electrons. In fact, valence band spectra appear at the lower binding energy region of XPS spectra. Nevertheless, irradiating the sample with UV photons instead of X-ray, dramatically increase the efficiency of the emission of VB electrons.

The use of an UV light source allows the characterization of the valence band of a solid with higher resolution than XPS. This characterization technique is called ultra-violet photoelectron spectroscopy. The photoemission process taking place in UPS is schematically represented in figure 9. The same as in XPS, it is based on an elastic process where the energy of the photons is transferred to the electrons. The energy of UV-photons is not enough to eject most of core level electrons, so the spectra is restricted to the valence band region.

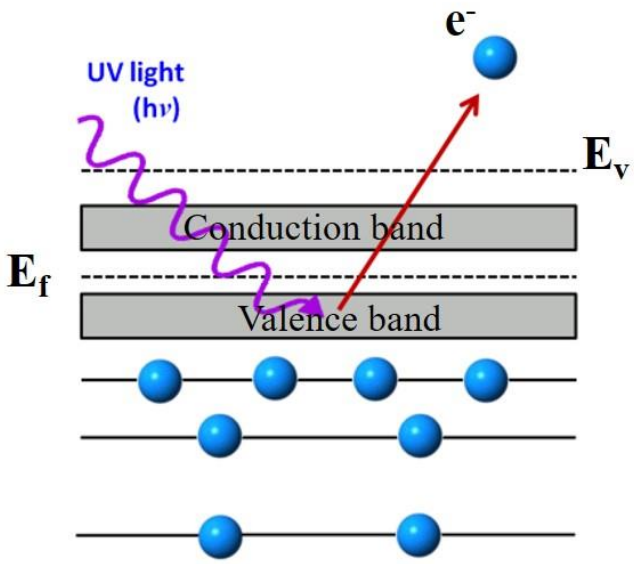

Figure 9. Schematic representation of Ultra-Violet Photoelectron Spectroscopy (UPS).

There are several models of ultra-violet lamps but the most used are the He lamps. The energies of the photons can be 21.2 eV for He I or 40.8 eV for He II.

Since UPS measures VB electrons, the information obtained from the spectra is completely different to thus obtained by XPS. The analysis of UPS spectra reveal information about the electronic structure of molecular orbitals directly involved in chemical bonding, and thus, about the electronic properties of solids, such as the work function.

One-step further, angle resolved photoelectron spectroscopy study the energy of the photoelectrons as a function of the angle. Two-dimensional detectors have been developed with this purpose, but it can also be done with a mono-dimensional one, rotating the sample and measuring at different angles. This technique reveals information about the momentum of the electrons, since electrons with different momentum will scape at different angles. The electronic structure of the VB, especially nearby Fermi level, determinates many properties of solids, hence the growing interest in this technique.

XPS

- Detection of core electrons.
- Elements at a surface and their chemical environment.

UPS

- Detections of VB electrons.
- Molecular orbitals, VB and work function of a material

Chapter 4. The photoelectron spectra

The first step of the standard protocol when analysing a sample by XPS consists in measuring the overview, also called survey or wide scan, covering a wide range of energies. It allows a fast identification of the elements at the surface of the samples and gives a first idea of their relative quantities. Then, the detected elements are measured in high-resolution, making visible the detailed shape of the peaks and slight shifts of energies. This way, high-resolution spectra of each of the key peaks allow the study of the chemical state and chemical environment of those elements.

Figure 10 shows the survey spectra obtained by XPS of two different samples: SiO_2 and silver.

Several features appear in XPS spectra:

- Background
- XPS peaks
- Auger Peaks
- Plasmons and satellites
- Valence Band

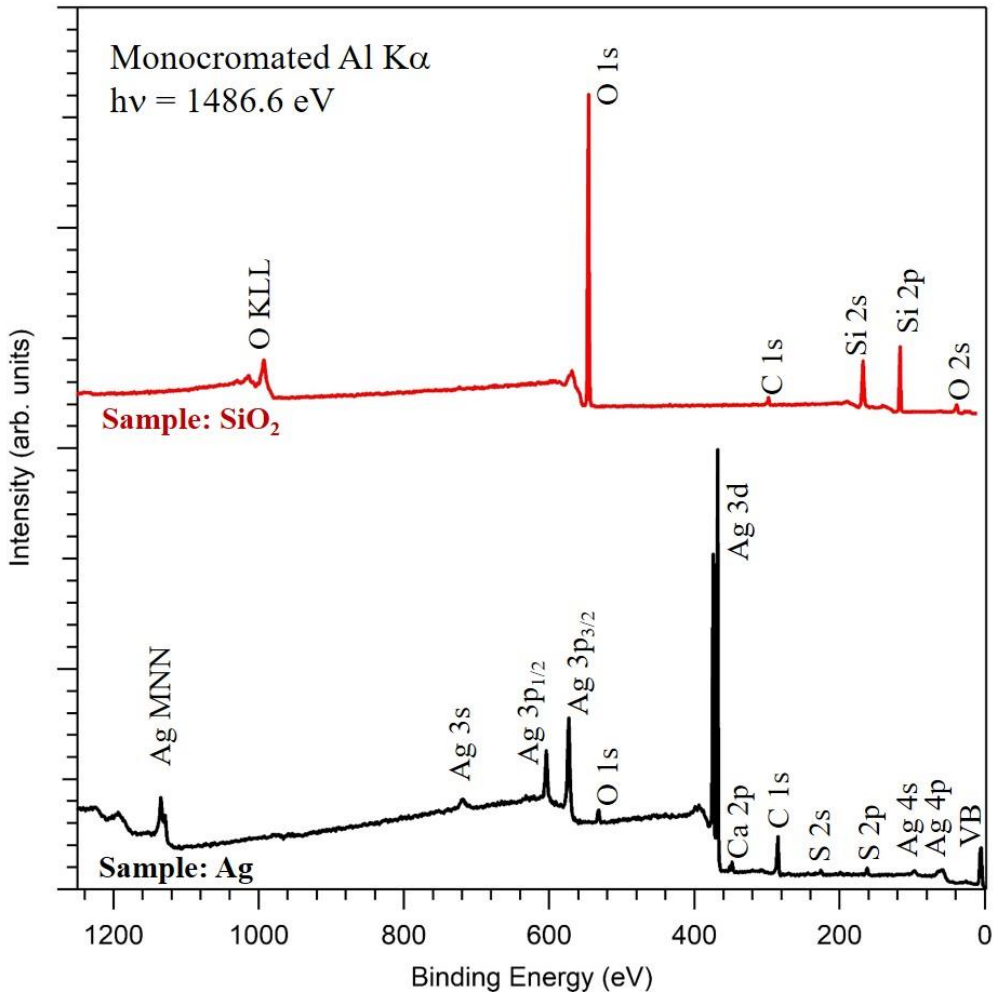

Figure 10. XPS spectra of SiO_2 (red) and Ag (black). It shows the full range of energy accessible by the Al Kα X-ray source. The figure shows the different XPS and Auger peaks as well as the VB.

The identification of the different peaks is done by comparing with previous experiments performed on reference samples. Thus, the spectra and energy values of pure elements as well as different compounds are available in databases and previous works. Notice, XPS spectra plots the amount of electrons reaching the detector as a function of the binding energy instead of the KE. This is due to the fact that BE does not depend on the energy of the X-ray photons, unlike KE does. This way it is possible

the comparison between samples measured by using different X-ray sources. It is just the opposite in the case of Auger peaks. Their KE is independent of the energy of the X-ray source, so Auger lines are usually referenced to their KE.

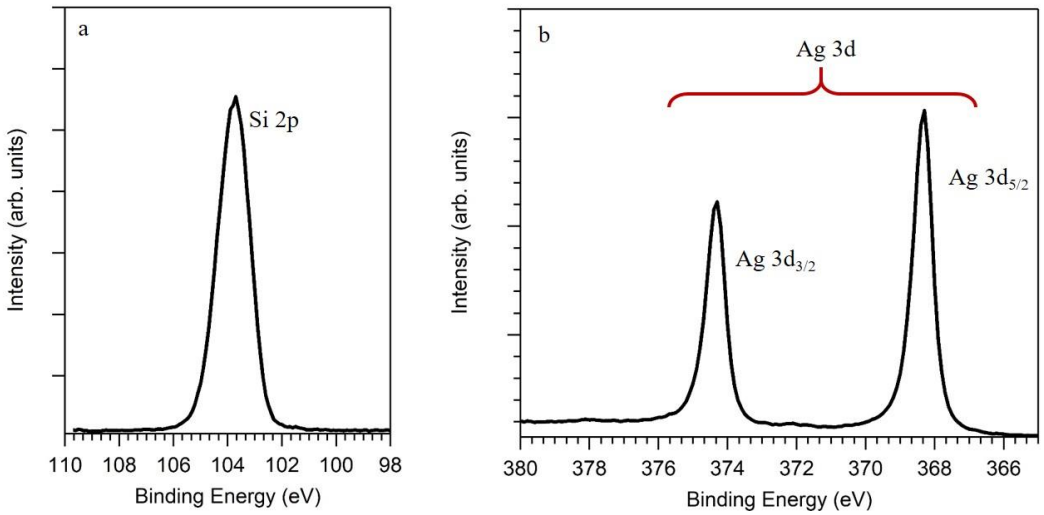

Figure 11. High-resolution XPS spectra of Si 2p (a) and Ag 3d (b) obtained from SiO_2 and Ag samples, respectively.

As we said before, the wide scan spectra is very useful for identifying the elements at the surface of the sample, but high-resolution measurements are necessary for assessing their chemical environment. We notice that each of the elements has several peaks, for instance Silicon has Si 2p and Si 2s core levels while Silver has Ag $3d_{5/2}$, Ag $3d_{3/2}$, Ag $3p_{3/2}$, Ag $3p_{1/2}$ and Ag 3s among others (figure 10). Nevertheless, in most of the cases it is enough to measure just one of the peaks to get the information of that element. Unless any overlapping problem, usually everyone measures the same peak for each element, chosen for reasons such as its higher intensity, narrower range of energies to measure or easier interpretation. Thus, by measuring Si 2p and Ag $3d_{5/2}$ core levels in high-resolution mode, it is possible to obtain the chemical information about the Silicon and Silver

atoms in the respective samples. Figure 11 shows the high-resolution spectra of Si 2p from a SiO_2 sample and Ag 3d core level from a metallic silver sample.

Finally, we remark the time needed for XPS measurements strongly depends on the composition of the samples. While the overview is typically obtained in a few minutes, sometimes much longer times are needed for measuring very low intensity peaks in high-resolution mode.

4.1. Background

The background in XPS is mainly due to inelastic interactions of photoelectrons that scape from the surface losing energy in the way. Several factors take part in its complex shape, both related to electronic effects in the sample and to the equipment. Baselines are drown as attempt to distinguish XPS peaks from other extrinsic phenomena. The most used line shape backgrounds in XPS are **linear, Shirley and Tougard** backgrounds:

- **Linear** background (figure 12a) is constructed by drawing a straight line between the experimental data available at higher and lower energies than the XPS peak. It is the simplest background that can be used in XPS peaks.

- More commonly used, a **Shirley** background (figure 12b) consist in an algorithm that tries to simulate a step function that appears in XPS peaks. Figure 12b shows a Shirley background under an Ag 3d peak of a silver sample.

- **Tougard** background takes into account the probability of energy loss events.

Moreover, in some cases a combination of backgrounds can be used, or even the inclusion of cubic spline polynomials to increase the flexibility of the shape line. As general rule, the selected start and end data should be far enough from the centre of the XPS peak. Special care should be taken with noisiest spectra, where the selection of these points can largely alter the line, and thereby the area under the peaks.

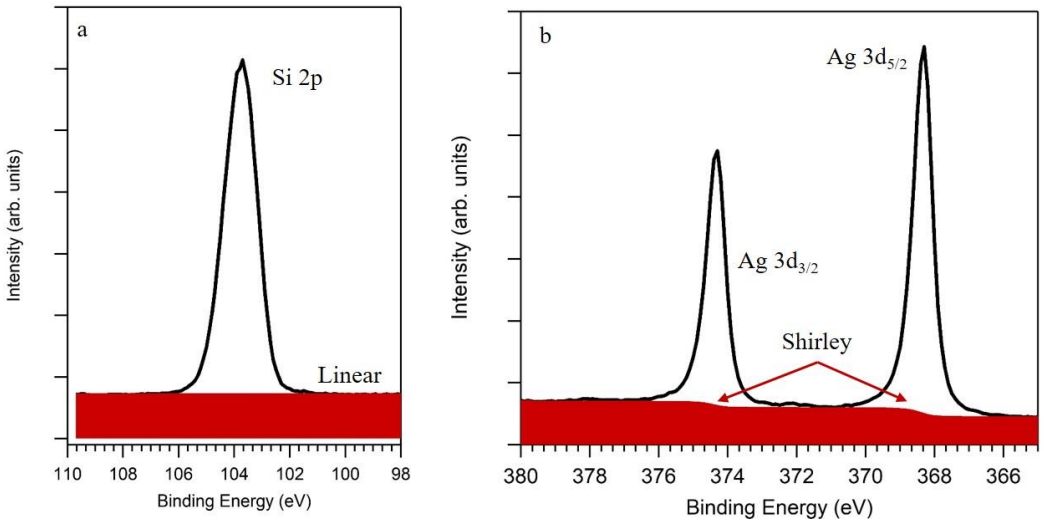

Figure 12. Linear (a) and Shirley (b) backgrounds used in XPS.

4.2. XPS peak

XPS peaks present a complex shape due to the physics involved in the ionization process of the atom and ejection of the photoelectron. Nevertheless, in the simplest case of symmetric peaks, it is possible to have a good approximation to the peak shape by using a Voigt function, *i.e.* a convolution between a **Lorentzian** and a **Gaussian** functions.

- Lorentzian function: lifetime broadening of the core level
- Gaussian function: experimental broadening, more related to the quality of the system: analyzer, monochromatic X-rays, etc.

Moreover, some elements show asymmetric peaks, with a kind of tail at the higher BE side. In these cases, mathematically curved line shapes (asymmetric) are used for fitting.

As an example of the functions used for fitting an XPS peak, figure 13 shows the Mo 3d core level measured from a MoO_3 thin film on a SiO_2 template. The best fit is also included. There are special programs that facilitate the fitting of the spectra. The first step is to draw the background, a Shirley background in this case. Then the components are included, with a fixed combination of Lorentzian and Gaussian functions. The software optimize the parameters involved in the fitting, such as the position of the peaks, their Full Width at Half Maximum (FWHM) and their area. It is important to keep in mind it is a mathematical optimization. Thereby, in some cases it is necessary to include some constrains to the parameters in order to achieve a fit in good agreement with the chemistry of the sample. For example, in cases like this with a doublet of peaks, Mo $3d_{5/2}$ and Mo $3d_{3/2}$, due to the spin orbit splitting phenomenon, we can include indications about the distance between peaks, the ratio between their areas and the FWHM between the peaks. The curve at the bottom of the figure represents the error between the experimental raw data and the fitting.

By comparing the parameters, especially the position of the peaks, with previous works, it is possible to ascribe the spectra of figure 13 to Mo atoms in a MoO_3 chemical environment (Mo^{6+}).

The shift of binding energy depending on the chemical bonding is the key to find out the local chemical environment of the elements at the surface

of the sample. As indication, chemical bonding withdrawing electronic charge from the valence band use to shift the binding energy to higher values. On the contrary, interactions increasing the electron charge in the valence band change the binding energy to lower values. The spectra become more complex when elements have a mix of oxidation states or chemical environments. When the difference between their binding energies is lower than the resolution of the equipment, it is obtained separates peaks but a convolution of them.

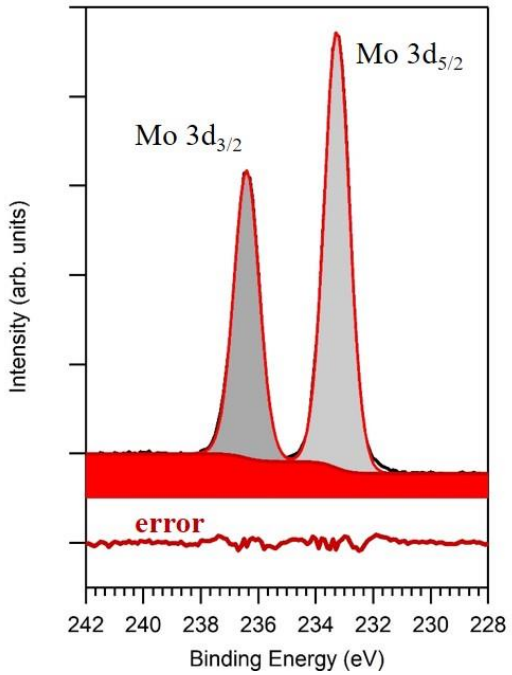

Component	$Mo3d_{5/2}$	$Mo3d_{3/2}$
LG (%)	30	30
BE (eV)	233.3	236.4
FWHM (eV)	1	1
Area (%)	60	40

Figure 13. XPS peak of Mo 3d and its fit. The table on the right shows the key parameters obtained from the fitting.

4.3. Auger peaks

As it was previously described, by doing XPS, Auger electrons are also emitted by the sample and thus, they appear in the spectra. Figure 14a shows the XPS overview of a graphene sample on a copper foil obtained by a monochromatic Al Kα X-ray source. As it is expected, Cu 2p XPS peak (substrate) as well as C 1s (graphene) appear in the spectra. Moreover, a large feature composed by several peaks appears at energies ranging from about 530 eV to 760 eV. This large feature is the Cu LMM Auger peak. More in detail, Figure 14b shows a zoom in of the most relevant part of the Auger peak.

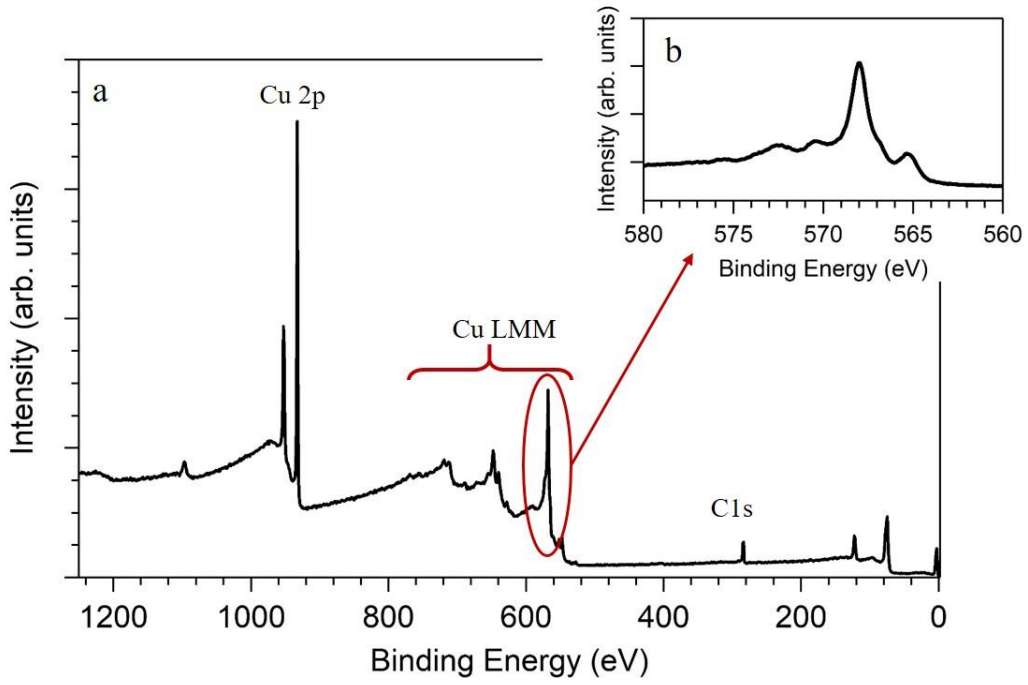

Figure 14. XPS spectra of a graphene sample on a copper foil. a) Overview and b) Cu LMM Auger peak.

The shape of Auger peaks uses to be complex and span through large energy regions. High-resolution measurements of Auger peaks also render information for elemental identification and chemical state analysis, but

their interpretation is usually more complex than that of XPS peaks. However, there are some elements where the discrimination between some chemical states is clearer by Auger spectra than by XPS peaks.

4.4. Other features

There are several features, due to different phenomenon, that can appear in XPS spectra. They should be taken into account for its interpretation.

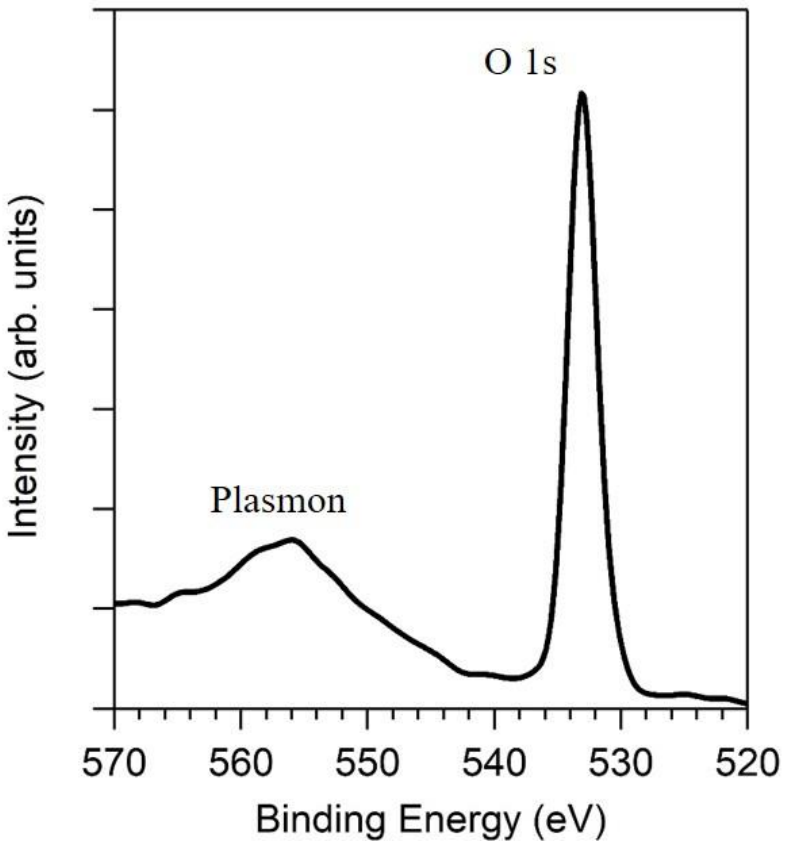

Figure 15. XPS spectra of MoS_2 on SiO_2. The figure shows the O 1s XPS peak and its associated plasmon (energy loss)

A plasmon peak is related with an energy loss phenomenon. As it was previously described, inelastic scattering of photoelectrons traveling through the sample shapes the background. When there is higher probability of certain interactions, such as with a collective oscillation of electrons, more photoelectrons loss uniform amounts of kinetic energy, generating peaks. Plasmons appear at higher binding energy than the XPS peak. Figure 15 shows the O 1s XPS peak and the associated plasmon of a MoS_2 film on SiO_2 sample. Plasmons can be attributed to the bulk or to the surface of a material and thus, sometimes they appear separated in the spectra.

Other possible features are the shake-up peaks, caused by excitation of valence band electrons due to the photoemission process. This phenomenon is typical in paramagnetic compounds of transition metal oxides as well as in organic species with coordinated double bonds, such as graphene, due to $\pi \rightarrow \pi^*$ excitations. When valence band electrons are released instead of excited then it is called shake-off.

Non-monochromatic X-rays sources also produce satellite peaks. Minor X-rays lines irradiates the sample along with the main line. If their energy is enough to eject photoelectrons, then causes repeated peaks in the spectra. The difference of binding energies between duplicates is the difference between the energy of the X-ray photons. Their intensity is much lower than the main XPS peaks.

4.5. Valence Band

The valence band appears at the lower binding energy range of the XPS spectra. Typically, its energy is lower than 16 eV. Nevertheless, UPS obtains higher resolution spectra of this region by using a ultra-violet lamp.

Valence band spectra measured by UPS can show differences compared to XPS. It is not only due to its higher surface sensitivity, but also because photons of different energy can excite different electronic transitions with different probability.

Figure 16 shows the valence band of Ag(111) single crystal. The spectra was obtained with a He I lamp in which the energy of the photons is 21.2 eV. This lamp has several advantages with respect the X-ray photon source. On one hand, its energy is close to the valence band energy. On the other, its resolution is up to three times higher than the X-ray source. Moreover, its intensity is also much higher allowing a fast measurement.

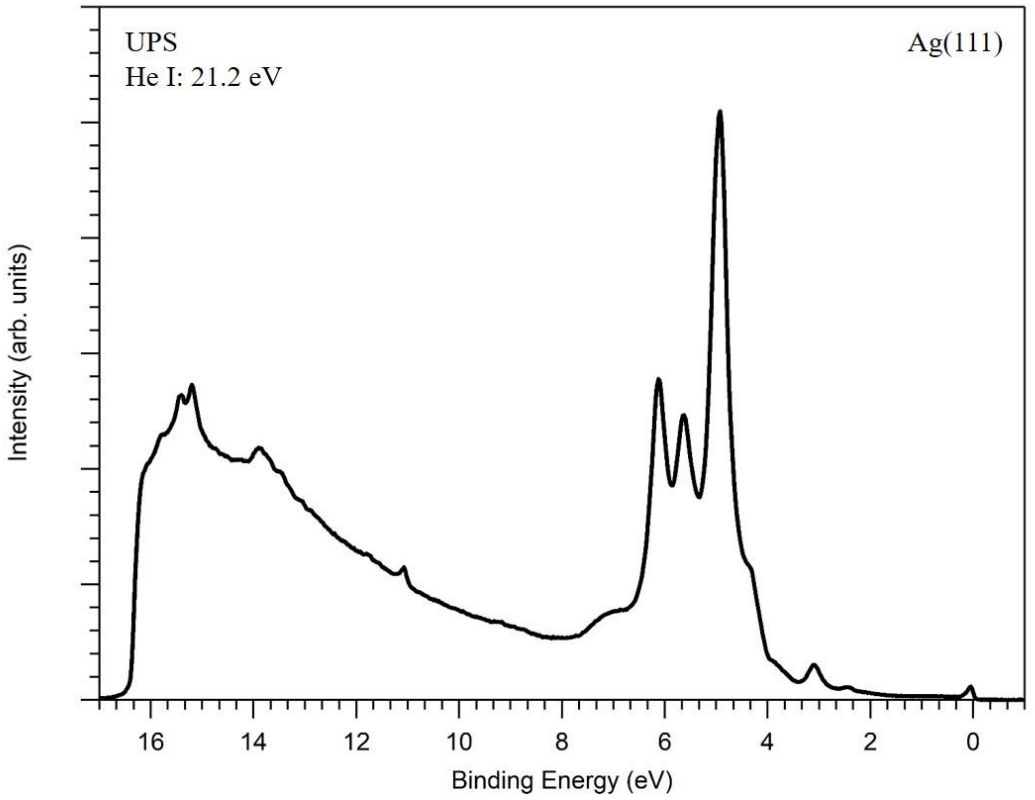

Figure 16. UPS spectra of Ag(111). Energy of the photons 21.2 eV (He I)

Valence electrons come from orbitals with higher hybridization degree, related to the chemical bonding. The resulting spectrum show a more continues structure rather than separated peaks, complicating the analysis.

Finally, just to point out a couple of useful features in the spectrum: the energy of the cut off ($E_{cut\ off}$), given by the intensity drop at higher BE, and the Fermi edge (E_F), from where the emission of electrons starts. The work function of the sample (Φ) can be calculated by using these data and equation 2:

$$\Phi = h\nu - (E_{cut\ off} - E_F) \qquad \text{Eq. 2}$$

4.6. Quantification

The area of an XPS peak of a specific element is related with the number of atoms of this element. Thus, as much atoms of an element are at the surface of a sample, higher will be the area of its XPS peaks. Nevertheless, it is not possible to do an absolute quantification of the elements. Rather than this, XPS provides a method for knowing the relative quantity between elements at the surface of a sample. The key idea is to measure the different elements that appear in an overview and compare their areas. It is important to remark that for doing quantification in XPS every element must be measured with the same experimental conditions, *i.e.* the power of the X-ray source as well as the operating mode of the spectrometer have to be the same during the measurement of the different elements.

Moreover, other factors have to be taken into account for quantifying an XPS spectra: the **cross-section** or sensitivity factor of the elements and the **transmission** of the spectrometer. The cross-section is the probability of

emission of a photoelectron from a specific element and core level upon irradiation with X-ray. Nowadays, the cross-section of each of the levels of each of the elements are available in databases. The transmission of the spectrometer is a function that characterize the specific machine used for measuring the sample. Roughly, the efficiency of the machine for detecting electrons with different energy is different and thus, this efficiency has to be corrected for quantifying the area of the XPS peaks.

Firstly, we discuss the case of a sample with just two elements A and B. Equation 3 shows the relation between the elements:

$$\frac{\#A}{\#B} = \frac{I_A/(\sigma_A \times T_A)}{I_B/(\sigma_B \times T_B)} \qquad \text{Eq. 3}$$

Where #A and #B are the quantity of atoms A and B, I_A and I_B are the area of the XPS peaks, σ_A and σ_B are the respective cross-sections and T_A and T_B are the transmission function at the energy of the peak A and B, respectively.

Moreover, equation 3 can be generalized to a case of n elements (equation 4):

$$A\ at.\% = \frac{I_A/(\sigma_A \times T_A)}{\sum_n I_n/(\sigma_n \times T_n)} \times 100 \qquad \text{Eq. 4}$$

Where A at. % is the atomic % of element A, I_A is the area of the XPS peak of the element A, σ_A is its cross-sections, T_A is the transmission function at the energy of the peak A and I_n, σ_n and T_n are the respective parameters for every element detected in the sample.

This way, it is possible to know the atomic % of each of the elements or equivalently, the stoichiometry of a sample. Keep in mind that this number is just an approximation. Factors such as the decay of signal intensity from

an element with the depth and the inaccuracy drawing the background add error to the quantification.

4.7. Binding Energy correction

In previous chapter, we have seen that the electron energy analyzer measures the kinetic energy of the photoelectrons and then, by using the equation 1 it is possible to calculate the binding energy of the spectra. Although the equipment is correctly calibrated, it can be originated an energy shift in the spectra due to different processes as it can be the accumulation of electronic charge in the sample. During XPS measurements, the samples are losing electrons. They are connected to an electrical earth in order to recover the neutrality, but it depends on the electrical conductivity of the samples. If the sample cannot recover all the missed electrons, it is generated a surface positive charge, causing shifts to higher binding energy values. Then, a further calibration has to be performed.

In some special samples, as is the case of metals, the binding energy can be fine calibrated by measuring the fermi edge of the spectra. Then the fermi edge is aligned with the cero of the binding energy. Figure 17a shows an aligned fermi edge of a copper sample.

In other cases, when lacking of a known sample to measure as reference, adventitious carbon contamination is commonly used for calibrating the binding energy of spectra. Nowadays, most databases use a value of 284.8 eV for C sp^2 from adventitious carbon as a reference. This number, although not strictly precise for every element, is a convention to facilitate the comparison. Hereby, when comparing results with previous works it is important to check the value the authors used for calibration. Figure 17b

shows an example of a MoS_2 sample in which C 1s is chosen for the energy calibration. The main C 1s peak is ascribed to C sp^2 (contamination) and shifted to 284.8 eV.

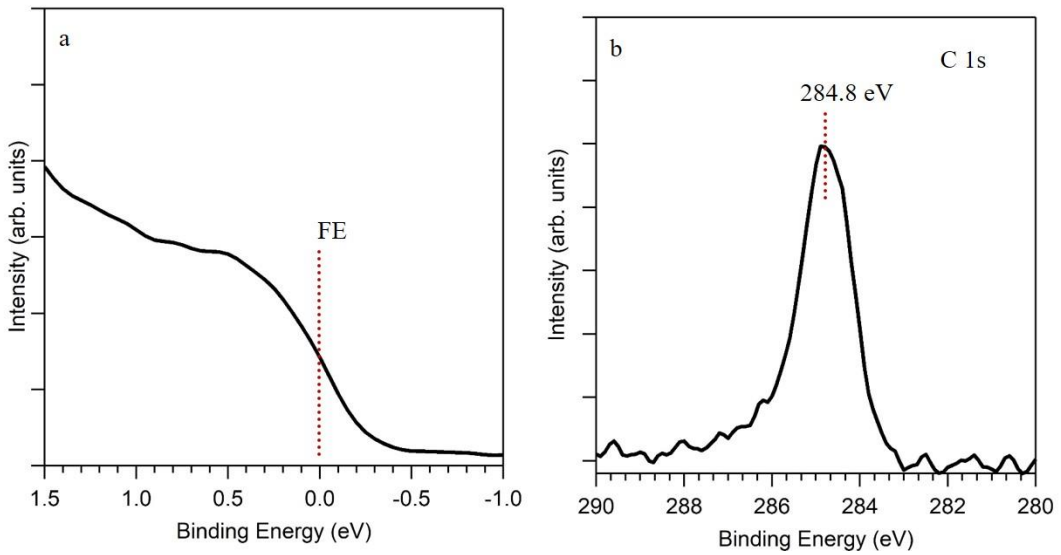

Figure 17. Binding energy calibration by using the fermi edge (a) and the C 1s core level of adventitious carbon (b).

Importantly, when a calibration for the energy is selected every peak of the XPS spectra has to be accordingly shifted. In the last case, a shift of -0.3 eV was used for correcting the C 1s core level. Thus, the same shift was applied to the other elements of the MoS_2 sample, *i.e.* Mo 3d and S 2p.

The measurement of some semiconductors and insulators leads to no uniform surface charge in most of the cases. It causes distortion of the peaks besides binding energy shifts. In these cases, it is necessary to inject electrons using an electron flood gun for charge compensation. The counterpart is that both the difficulty to exactly compensate the charge and the effects of the electron flood on the sample usually widens the spectra. Anyway, this procedure greatly expands the range of sample that can be measured by XPS.

Chapter 5. Surface sensitivity and depth profile

XPS is a surface technique, characterizing just the last few layers of the material. This important fact is due to the short distance that electrons can travel in a solid without suffering any interaction. Figure 18 shows the electron mean free path as a function of the electron energy in a solid. By considering the typical energy of the ejected electrons in a laboratory XPS system, it is clear from figure 18 that the distance they can travel freely in a solid is just a few nanometers. Because of this, any deposited contamination, like atmospheric contamination, strongly affect the spectra. As an example, figure 19 shows the comparison between the XPS spectra of a Ni sample measured before and after cleaning. The difference in the intensity of the Ni peaks in both spectra clearly indicates how carbon contamination largely affects the signal. Importantly, the nickel sample showed in figure 19 was cleaned *in situ* under ultra-high vacuum conditions and measured just after the cleaning process. If the sample is again exposed to atmospheric conditions, a reactive sample like nickel will oxidize and adsorb contamination at its surface in just few seconds.

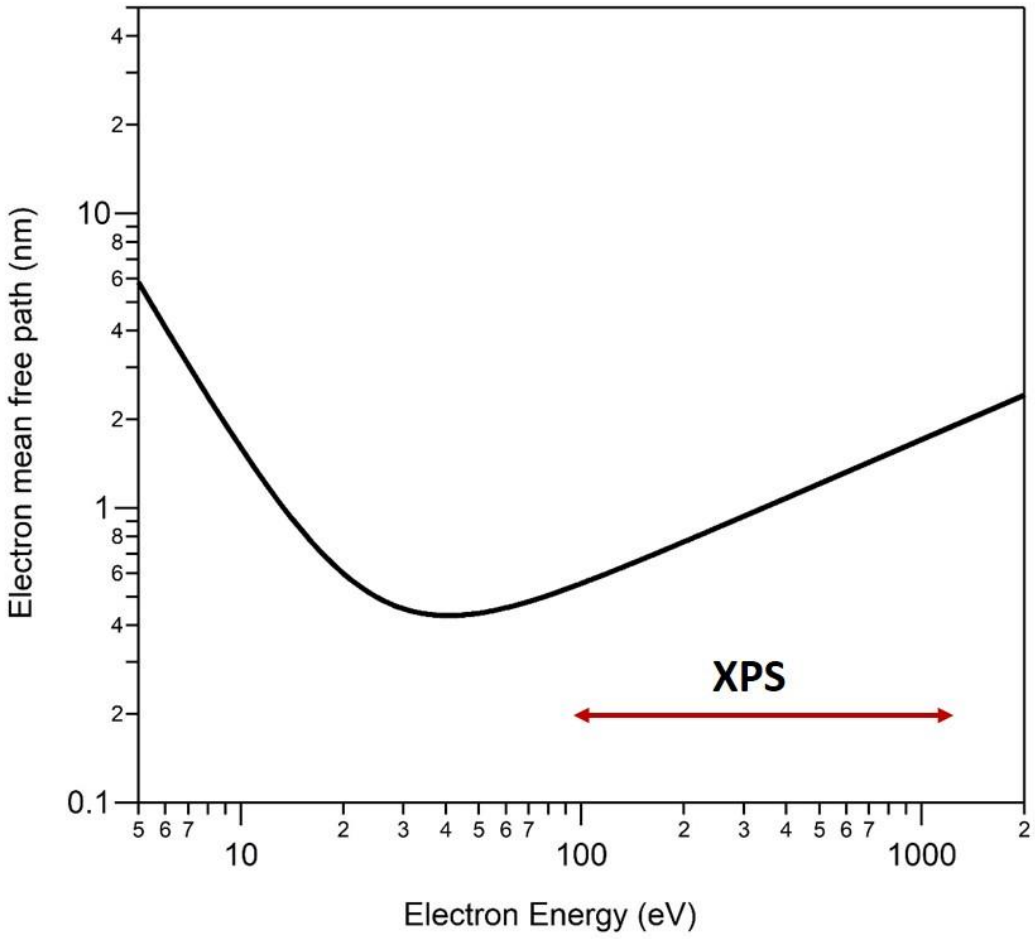

Figure 18. Electron mean free path vs electron energy in a solid.

A XPS photoelectron can travel just a few nanometers without losing energy in a solid.

XPS characterizes the last few layers of a material

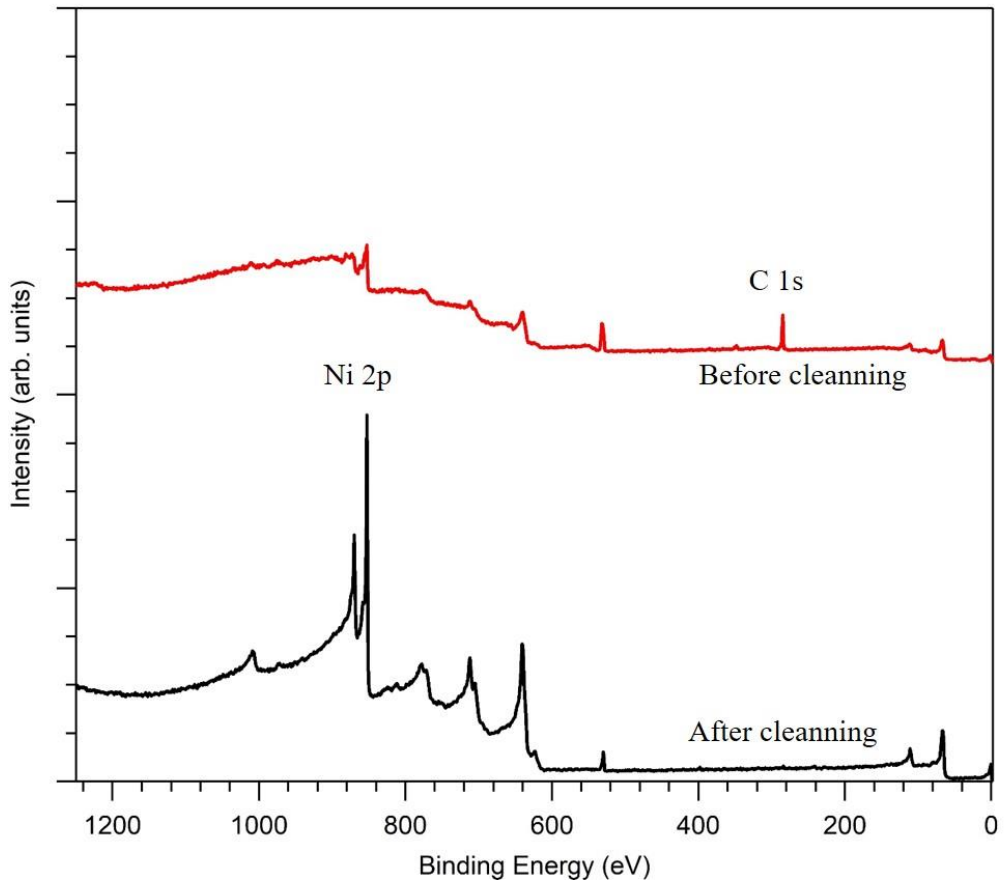

Figure 19. XPS spectra of a nickel sample before (red) and after (black) cleaning its surface.

Although XPS characterize just the last nanometers of a sample, there are some useful tools that allow measuring the underlying layers. The most important is the XPS depth profile by ion sputtering, discussed in the following sections.

5.1. Sputtering by Ar ions.

By irradiating a sample with high-energy ions, usually Ar^+, it is possible to remove some material from its surface. This way, the underlying material is exposed. Figure 20a shows the set up used to perform ion sputtering in an XPS system.

Several parameters affect the sputtering power: the element used as projectile, its energy, the angle between the sample and the ion beam and the chemical composition of the sample, among others. The table on figure 20 shows a typical set of parameters used in an XPS laboratory for doing ion sputtering. By fine-tuning these parameters, it is possible to remove material from the sample layer by layer. The main applications of this tool are cleaning and depth profile, but it is also useful for other purposes like to create reactive sites at the surface of a sample

Ion sputtering removes material from the surface of a sample.

It is a destructive technique!

A very important fact is that ion sputtering is a destructive technique. It works by removing material from the sample. Moreover, the sputtering shield is characteristic of each element, *i.e.* some elements leave the sample faster than others, and hence it can change the stoichiometry of the sample. For example, ion sputtering could causes reduction of oxides. This critical behaviour has to be seriously considered depending on the nature of the sample. This way, ion sputtering is very useful for removing surface contamination from pure metals, but inadvisable for mixed compounds such as oxides. Additionally, the softer is the material, higher is the damage caused to the sample. A progress in this respect has been the development of gas cluster ion guns. The clusters of gas atoms hit the sample with less energy than ions. It minimizes the damage and allows etching soft materials such as polymers.

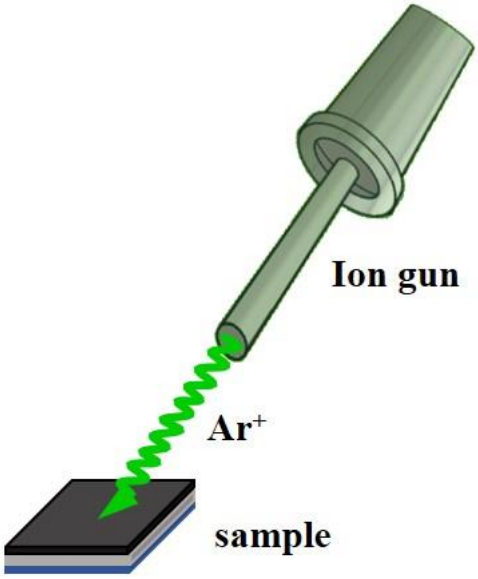

Projectile	Ar+
Energy	1 – 3 KeV
Angle between sample and beam	30 – 45°

Figure 20. Experimental set up used for doing ion sputtering. The table shows a standard set of parameters used for doing sputtering with argon for cleaning the surface of a metal.

5.2. XPS depth profile

By combining ion sputtering with XPS it is possible to do XPS depth profile, *i.e.* to analyse the composition of the sample as function of the depth. The diagram of figure 21 shows the sequence of XPS and ion sputtering required to perform depth profile.

Starting with a fresh sample, XPS spectra is first acquired. Then, cycles of sputtering and XPS measurement are repeated n-times until reaching the desired depth in the sample.

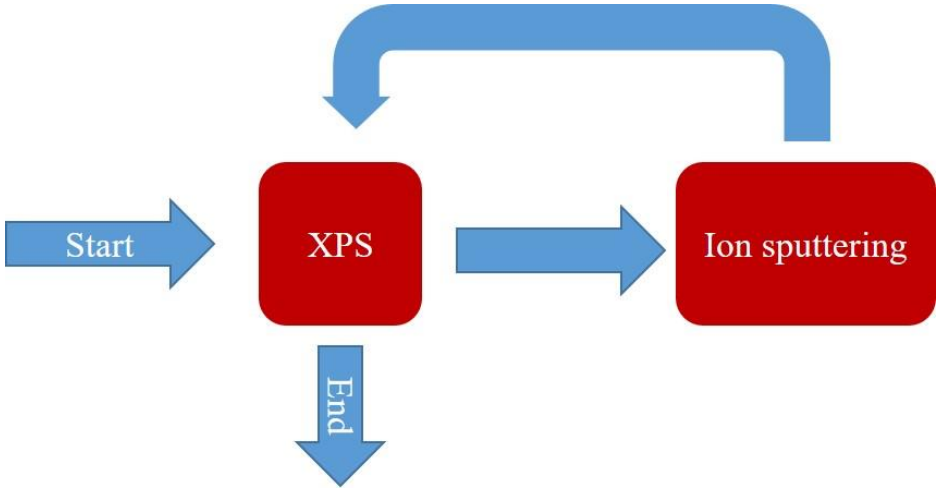

Figure 21. Diagram showing the experimental steps to perform XPS depth profile.

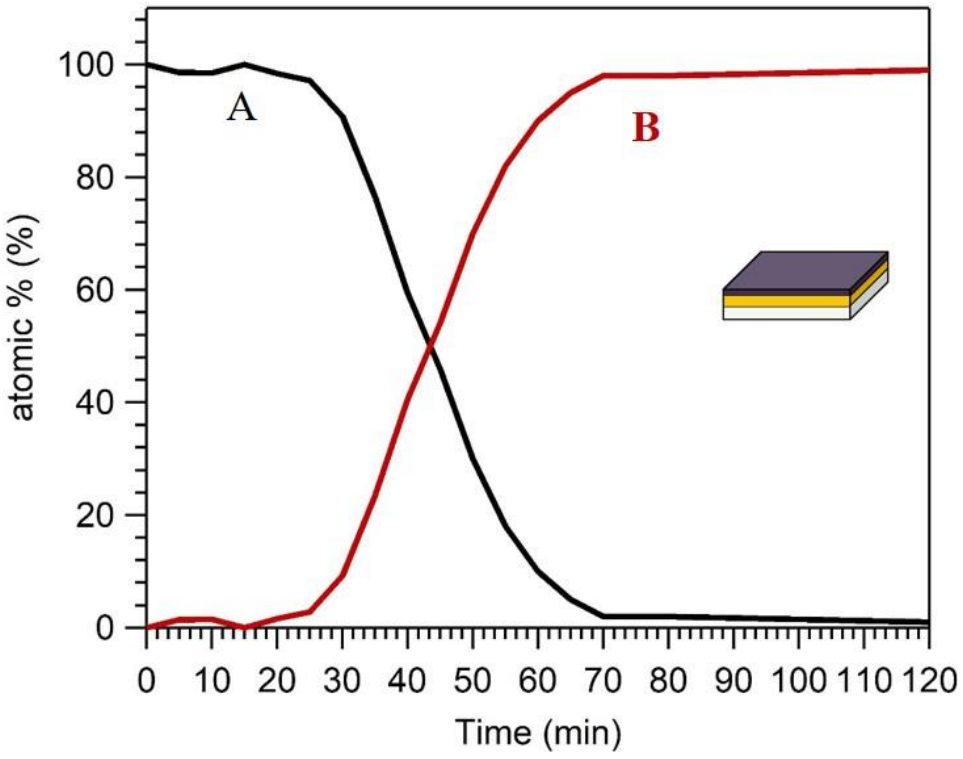

Figure 22. XPS depth profile of vertical stacked thin films. The hypothetical element A, the top layer, is on the hypothetical element B.

XPS depth profile is a destructive technique. Once a sputtering cycle is performed the XPS spectra comes from a depth of the sample not accessible before. This technique can be very useful for characterizing some materials, such as multi-layer samples, although it could change the stoichiometry of the compounds. The inset of figure 22 shows a vertical hetero-structure formed by two thin films of arbitrary elements on a template. If the top film is thicker than the depth analysed by XPS, the second one is not accessible by standard XPS. Nevertheless, removing layer by layer the material of the surface opens the way to measure the lower film.

Figure 22 shows the normalized curve obtained by measuring the area of the XPS peaks ascribed to element A (grey thin film) and element B (yellow thin film). At the beginning, only the outer thin film is detected, but after several cycles of sputtering, element B appears in the XPS spectra while element A slowly disappears.

XPS depth profile consists in doing XPS while removing material from the surface sample.

It is a destructive technique

5.3. Non-destructive depth analysis

This technique allows a depth analysis of the few top nanometers that XPS can measure. It compares spectra obtained by rotating the sample with respect to the detector. In XPS, the intensity of electrons from the surface as a function of the emission angle is described by equation 5.

$$I = Io \exp\left(-\frac{d}{\lambda * Cos(\theta)}\right) \qquad \text{Eq. 5}$$

Where Io is the intensity from a uniform thick film, d is the depth of the emitted electrons, λ is the mean free path and θ is polar angle.

Usually XPS is performed at normal emission take off angle, *i.e.* θ=0º (figure 23a). The more the angle increases, the greater the sensitivity of XPS to the surface. By acquiring XPS spectra with a high angular resolution at a high angle, *e.g.* at θ=70º, the analysis will be extremely sensitive to the surface (figure 23b).

XPS vs polar angle is a non-destructive technique.

It is useful for studding thin films

Thus, a set of XPS spectra as a function of the polar angle is quite useful for samples such as thin films of a few nanometers on different substrates. On one hand, at normal emission both the thin film as well as the underlying substrate will appear in the XPS spectra. On the other, at higher polar angles, the information obtained by XPS will mainly come from the mostly external thin film.

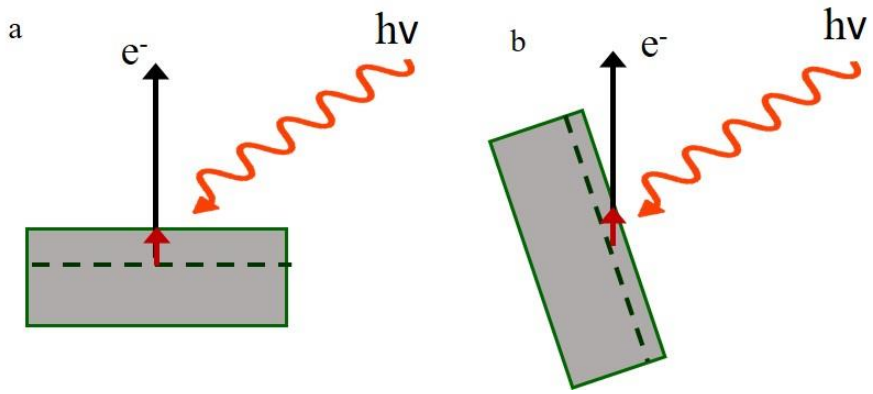

Figure 23. Electron emission at different angles. (a) Normal emission and (b) at a high polar angle.

Chapter 6. Applications of XPS and examples

This chapter discusses different applications of XPS, but before this, it is important to remark the kind of samples that are accessible by XPS. The wide set includes, among others, thin films, powders, amorphous or crystalline samples, alloys, pellets, ceramics, geological samples, organic compounds. Figure 24 shows a set of photos of standard samples. Two things to take into account always are the size of the sample holder and make sure there are no residues that degas under ultra-high vacuum conditions.

XPS is compatible with a large set of samples:

- Thin films
- Crystals
- Powders
- Ceramics
- Biological samples

Figure 24a shows a photo of a thin film growth on a SiO_2 wafer. The uncovered region on the right is due to a mask used during the growth. This way, both the thin film as well as the SiO_2 template can be characterized with XPS at the same sample. Figure 24b shows a photo of a crystalline powder onto conductive carbon tape. This is a quite useful method of mounting samples for XPS. In other cases, it is better to disperse the powder in a good solvent and dry a drop on a template. Figure 24c shows an example of a powder deposited by this drop coating technique. A good chose of the solvent is a critical step, the most used are ultra-pure water, acetone or ethanol but of course, the solvent must not alter the sample. The last example, shown in figure 24d, is a ceramic fixed to a sample holder by tantalum wires.

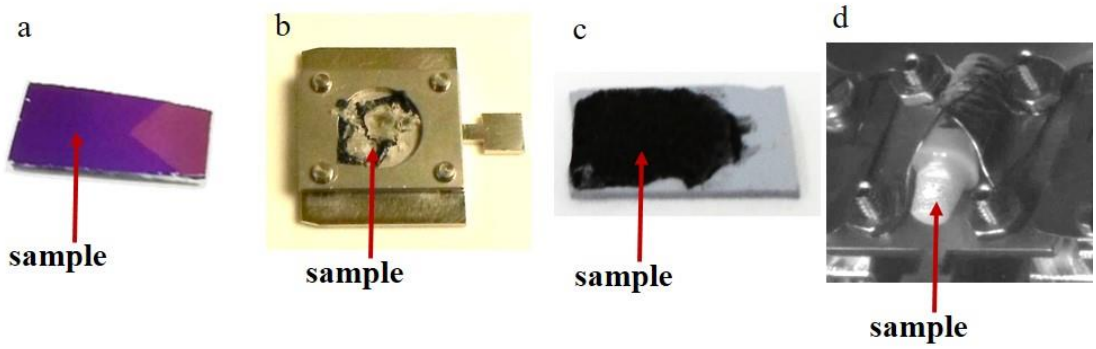

Figure 24. Photos of a standard XPS samples. a) thin films, b) crystals, c) powders and d) ceramic.

Modular UHV systems allows adding extra functionalities to XPS by upgrades. It was already mentioned some examples such as UPS with a UV lamp, AES with an electron gun, sputtering with an ion gun, among others. The flexibility of these systems also enables performing different experiments inside the equipment, before or during measurements. That includes, among others:

- Sample heating and cooling
- Variable angle sample orientation
- Dosing a sample with gases or vapours from materials by thermal evaporation. This allows following deposition or catalytic process at surfaces.

The key information obtained by XPS besides the flexibility of the UHV systems contribute to solve scientific problems from a wide diversity of fields, such as:

- Materials science
- Chemistry

- Physics
- Catalysis
- Biology
- Thin films
- Geology
- Energy
- Ceramic
- Mineralogy
- Polymers
- Environmental sciences

The following sections briefly show some examples of measurements carried out by XPS.

6.1. Graphene on copper

The first example is the characterization of a graphene sample growth on copper foil by chemical vapour deposition (CVD). Figure 25 shows the overview (figure 25a) and high-resolution C 1s core level (figure 25b) XPS spectra. All the features detected in the overview match with the main XPS and Auger peaks of copper and carbon, without any additional peak from contamination. For example, oxygen is one of the most common contaminants of the samples synthesized by CVD, but in this case, O 1s (near 530 eV) is not detected in the overview. Paying attention to the relative intensities of the main Cu peak (Cu 2p) and C 1s, as thicker the

graphene layer, more intense will be the C 1s signal while the Cu 2p signal will decrease.

The high-resolution C 1s spectra shows a sharp peak slightly asymmetric at around 284.5 eV. Both the binding energy value and the shape of the peak are in good agreement with the expected for a graphene sample [1-3].

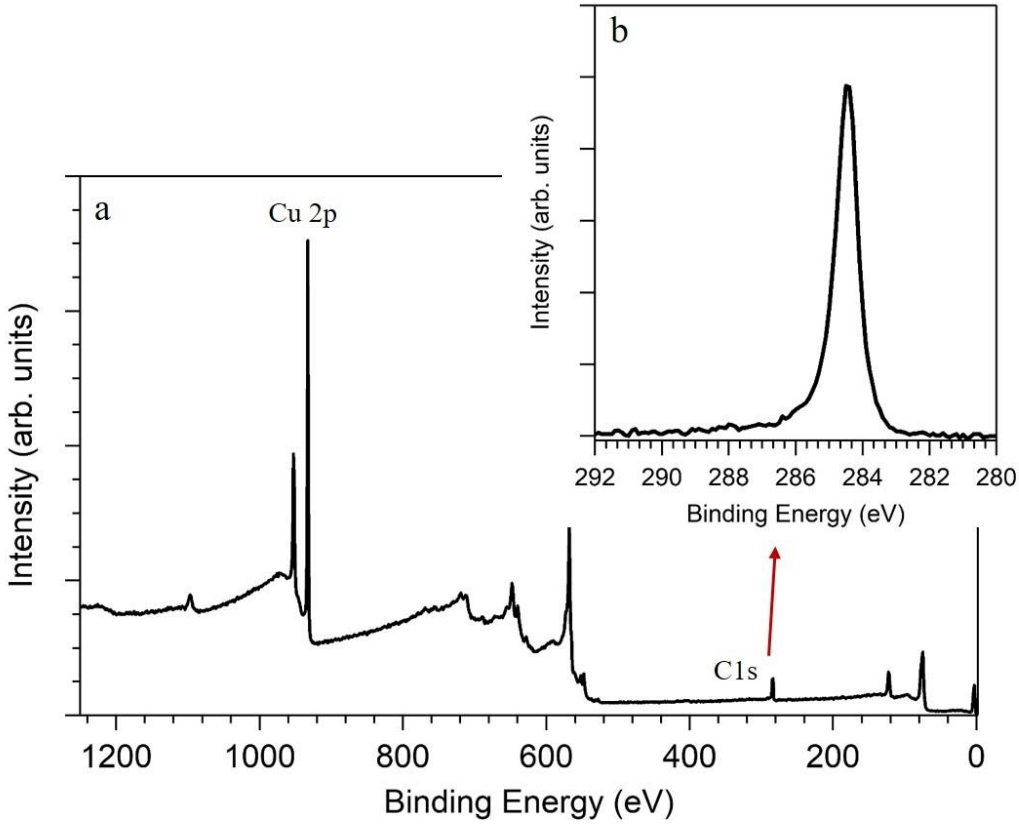

Figure 25. XPS spectra of graphene on copper. (a) overview and (b) high-resolution C 1s core level.

6.2. Characterization of the chemical environment of surface elements

XPS is very useful for characterizing the oxidation state and local chemical environment of the elements detected at the surface of a sample. In the following example, a thin film of MoO_3 is deposited on a SiO_2 wafer and then it is sulfurized by a chemical vapour deposition technique. The film was characterized by XPS before and after the sulfurization process for comparison.

Figure 26 shows the high-resolution XPS spectra of the main peaks of the key elements, molybdenum and Sulphur. Mo 3d and the S 2s (figure 26a) appears very close in energy, but barely overlap. The same happens in the case of S 2p and Si 2s (figure 26b).

XPS measurement of the MoO_3 film shows two sharp peaks in the Mo 3d region, corresponding to Mo $3d_{5/2}$ and Mo $3d_{3/2}$ spin orbital splitting (figure 26a, down). Mo $3d_{5/2}$ is centred at an energy of 232.9 eV, ascribed to Mo^{6+} [4-6]. In addition, figure 26b shows the Si 2s core level, from the SiO_2 substrate, without any trace of Sulphur.

The upper spectra of figure 26 show the results obtained after sulfurization of the film. Both Mo 3d peaks clearly shifted to lower binding energies, while a new peak appeared. Mo $3d_{5/2}$ is now centred at a BE of 229.3 eV. The new peak, at 226.5 eV is ascribed to S 2s core level. In parallel, two new peaks appear besides Si 2s, ascribed to S $2p_{3/2}$ (at 162.2 eV) and S $2p_{1/2}$ [6]. Thus, by combining all the information altogether it is possible to determine by XPS that the MoO_3 thin film was completely transformed in MoS_2.

XPS is useful for characterizing the chemical environment of the elements at a surface, and understand the changes produced by chemical reactions.

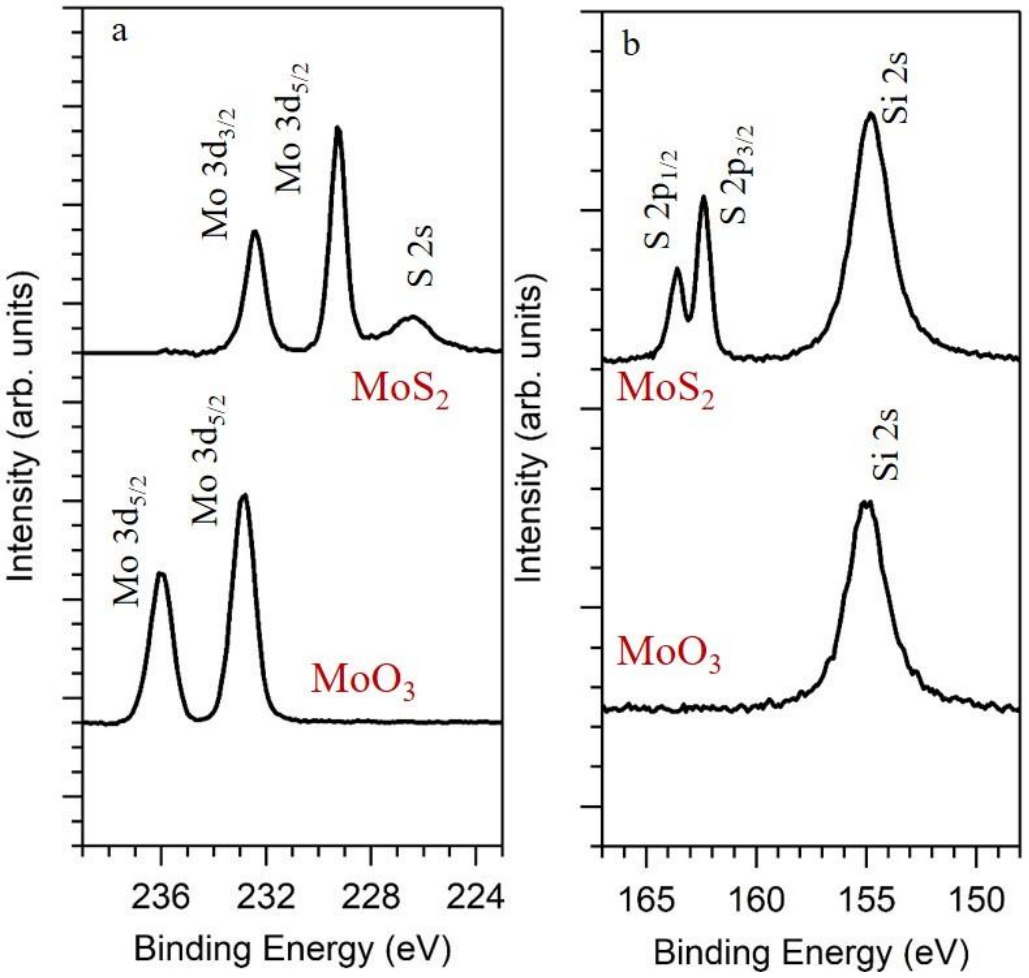

Figure 26. XPS spectra of Mo 3d (a) and S 2p and Si 2s (b)

6.3. Monitoring thin films growth

Figure 27 shows an example on how XPS can be used for monitoring the growth of a thin film on a substrate. In this case, platinum was evaporated onto a nickel sample. The experiment consist in repeated cycles of platinum evaporation and XPS measurement. This way, the growth of the platinum film can be followed as a function of the evaporation time or cycle.

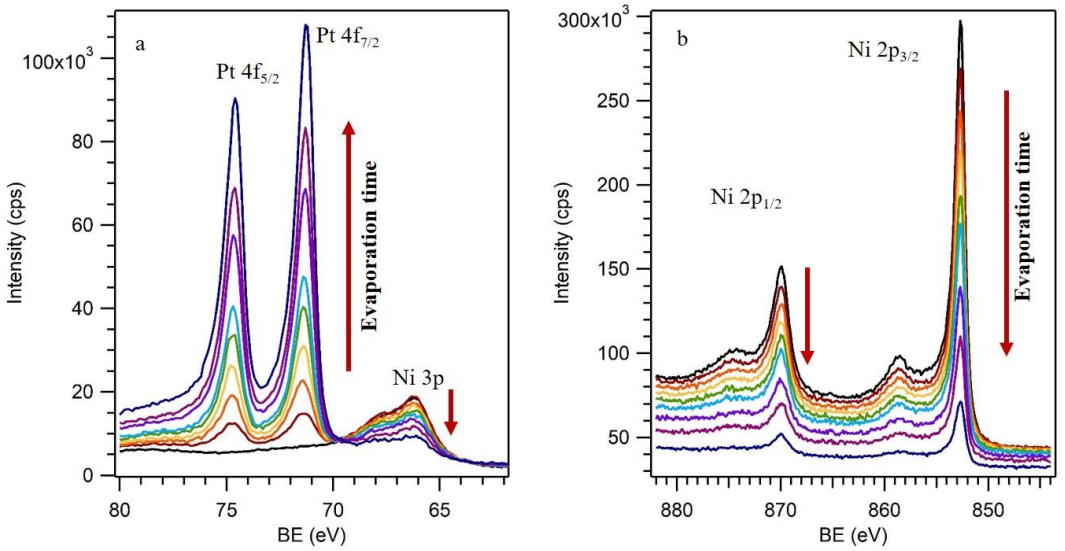

Figure 27. XPS vs evaporation time. a) shows Pt 4f and Ni 3p regions, while b) shows the Ni 2p region.

Figure 27a shows a series of Pt 4f core level spectra of progressive evaporation time. Moreover, in this region of energy, at lower binding energy, Ni 3p also appears. In a complementary way, figure 27b shows the XPS region ascribed to Ni 2p core level. The figures show how the platinum core levels, Pt $4f_{7/2}$ and Pt $4f_{5/2}$ increase as a function of the evaporation cycle while the peaks, Ni 3p, Ni $2p_{3/2}$ and Ni $2p_{1/2}$, decrease.

This way, it is possible to do a very good calibration of the platinum deposition as a function of the time. By fine-tuning the parameters of the evaporator, it is possible to control the quantity of platinum on the nickel surface, even at the sub-monolayer scale. Moreover, by measuring the binding energy of Pt $4f_{7/2}$ and comparing with already published results for platinum samples, XPS elucidates the chemical state of the platinum layer. In the present case, XPS shows a metallic platinum layer.

XPS is very useful for monitoring the growth of a sample on a template even at the sub-monolayer regime.

The use of XPS for monitoring the growth of thin films is not restricted to metals. Nowadays, it is also common to characterize the growth of a large set of materials on different templates such as organic thin films and graphene among others.

6.4. Following on-surface chemical reactions

This section shows the ability of XPS to monitor a chemical reaction. Figure 28 shows the XPS data of a thin film of graphene oxide (GO) on SiO_2 and the changes that occur upon heating the sample for reducing the GO.

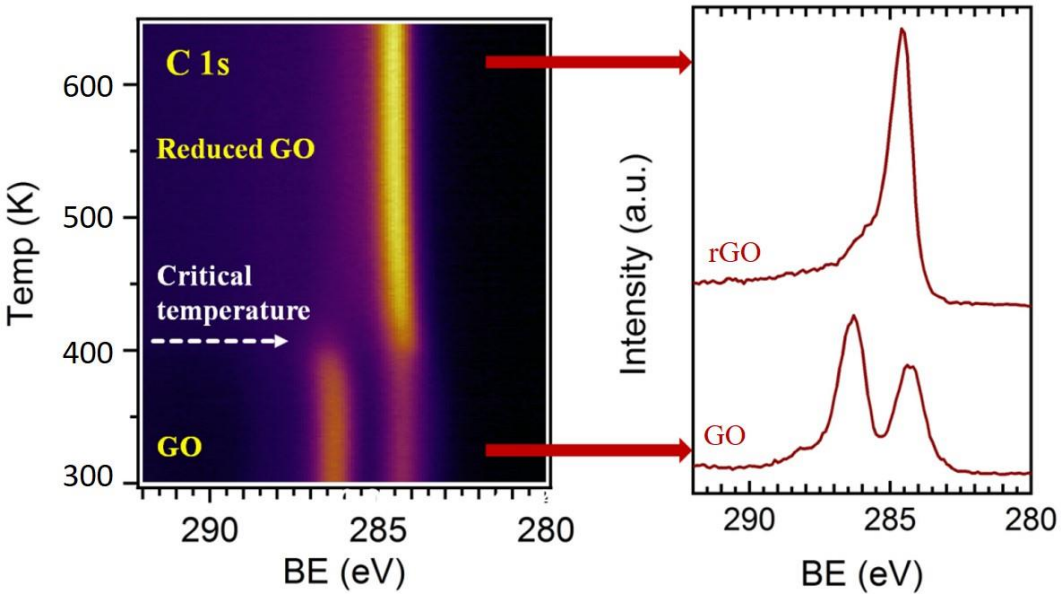

Figure 28. a) XPS spectra vs temperature. b) XPS of GO acquired at room temperature (bottom) and rGO acquired at a temperature higher than the critical (upper spectra).

Figure 28a shows a collection of hundreds of XPS spectra of the C 1s region. Each horizontal line of the picture is an individual spectra, where

the intensities are represented by colours. The y-axis indicates the temperature of the sample at which each spectra was measured. At room temperature, the C 1s core level shows the shape and BE values of a GO sample (figure 28b, down). The structure of C 1s peak of GO has several components. The first component, at lower BE, is ascribed to the non-oxygenated rings, *i.e.* C sp^2 net of graphene sheet with C sp^3 defects. The other components, at higher BEs, are ascribed to diverse oxidized species such as C-O-, C=O and COOH [7].

Once the sample is characterized at room temperature, a furnace installed at the bottom of the sample holder starts to slowly increase the temperature of the sample while doing XPS at the same time. The furnace is controlled by the computer and has a feedback circuit that allows maintaining a stable temperature during the XPS measurements. Thus, by fine controlling the annealing of the sample, it is possible to coordinate the acquisition of the XPS spectra with the temperature of the sample.

Figure 28a shows how the spectra drastically change after reaching a critical temperature slightly higher than 400 K. The peaks at higher BEs suddenly disappears while the peak at lower BE get brighter. The comparison of the XPS spectra obtained before and after the critical temperature (figure 28b, down and top, respectively) clearly shows the changes induced in the sample by the annealing. The strong signal from oxidized carbons of GO at room temperature enormously decreased after heating the sample. Accordingly, the XPS spectra of reduced GO (rGO) shows a sharper component ascribed to C Sp^2 as main feature.

This continous monitoring is not possible with many reaction, like wet chemistry or rections releasing dangerous products for the analyzer. The most usual analysis is done by comparison of the spectra at each step, or just before and after the reaction. Nevertheless, to acquire a set of XPS spectra vs temperature as the shown in figure 28a, following the reaction in real time, provides additional information. It makes possible to find a key parameter as the critical temperature and detect more subtle changes in the spectra around this point.

By synchronizing XPS with a parameter such as the temperature of the sample, it is possible to follow in real time the changes induced at the sample

6.5. Fitting examples

6.5.1. N 1s core level of melamine

Figure 29 shows the XPS spectrum of melamine molecules. The N 1s spectra of melamine has two components of similar intensity centred at binding energies of 399.9 eV and 399.0 eV. The component at higher binding energy is ascribed to the amino groups by comparing with previous works [8], while the second component corresponds with N atoms located in the s-triazine ring (Nsp^2) [9].

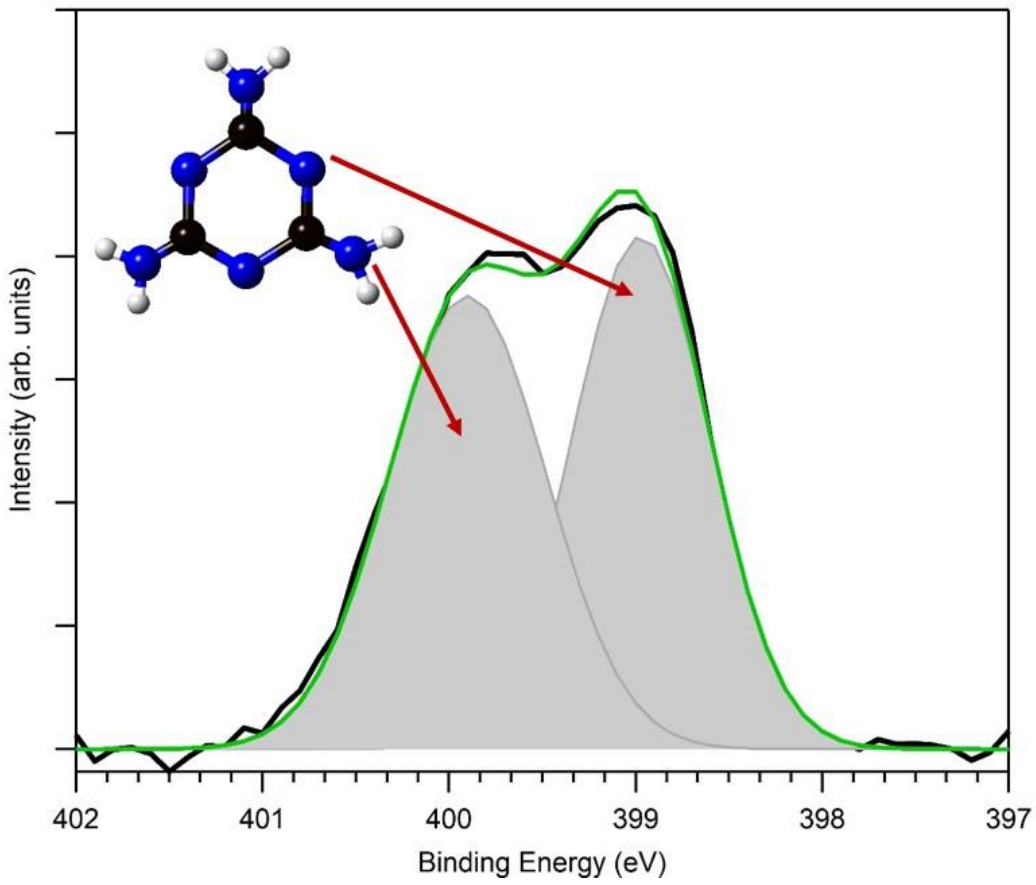

Figure 29. N 1s core level of melamine. The best fit is also included. Raw data is in black, background in red, synthetic components in grey and envelop in green. The inset show a ball and stick model of melanine.

In order to fit this spectra, first a linear background was used and then two components were introduced for obtaining a good agreement between the raw data and the envelop of the fit. The synthetic components are made by the convolution between a graussian and a Lorentzian functions, with a relative weight of 70:30 %. It is important to take into account that both components should have a similar full weight at half maximum value.

Moreover, from equation 4, and by using the areas of the two synthetic components, it is possible to know the relative quantities between the two

different nitrogens. This way, it was calculated a relative atomic percentaje between N atoms in the amino groups and in the s-triazine ring of aproximately 50:50 %. This result is in good agreement with the expected value for melanine, which has 3 nitrogen atoms in each of the both chemical environments.

6.5.2. Ti 2p core level of TiO_2

Figure 30 shows the Ti 2p core level of a TiO_2 sample. This core level shows two main peaks corresponding to the spin orbit splitting couple Ti $2p_{3/2}$ and Ti $2p_{1/2}$ levels. After drawing a shirley background, the spectrum was fitted using two components, centred at 458.6 eV and 464.3 eV, respectively. Both the BE values and energy difference between them are in good agrement with the energies expected for a TiO_2 sample[10,11].

The synthetic components have a relative weight of 2:1, typical for a 2p core level, although in the case of Ti 2p the couple have unqual FWHM values, being Ti $2p_{1/2}$ much shorter and wider than Ti $2p_{3/2}$.

Two extra feuatures appear in the spectra at higher binding energy, ascribed to energy loss plasmons.

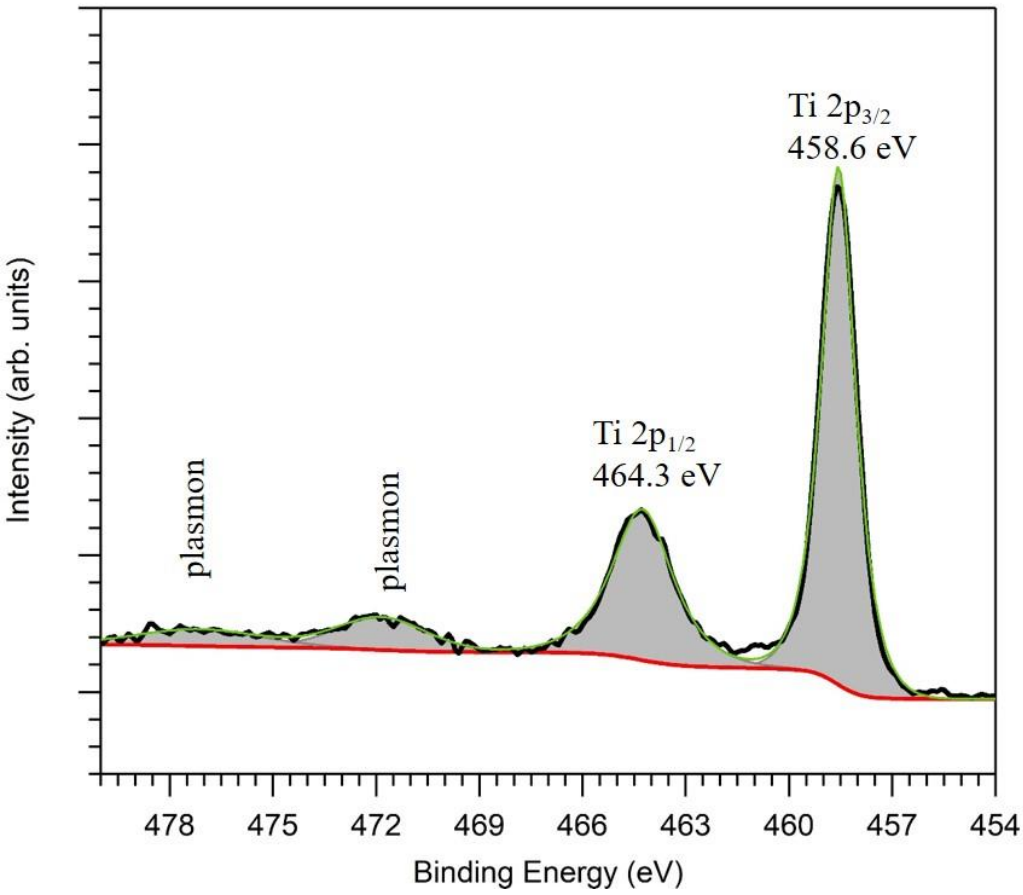

Figure 30. Ti 2p core level of a TiO_2 sample. The best fit is also included. Raw data is in black, background in red, synthetic components in grey and envelop in green.

6.5.3. Mo 3d core level from a Mo film partially oxidized and partially sulfurized

This section shows the basic rules for fitting XPS spectra in which several chemical environments coexists. This way it is possible to elucidate the different chemical species at a surface even in the case that the different components over-impose.

Figure 31 shows the Mo 3d region of a molybdenum thin film partially oxidized and partially sulfurized. We notice that S 2s also appears in the showed region, at a binding energy slightly lower than Mo 3d.

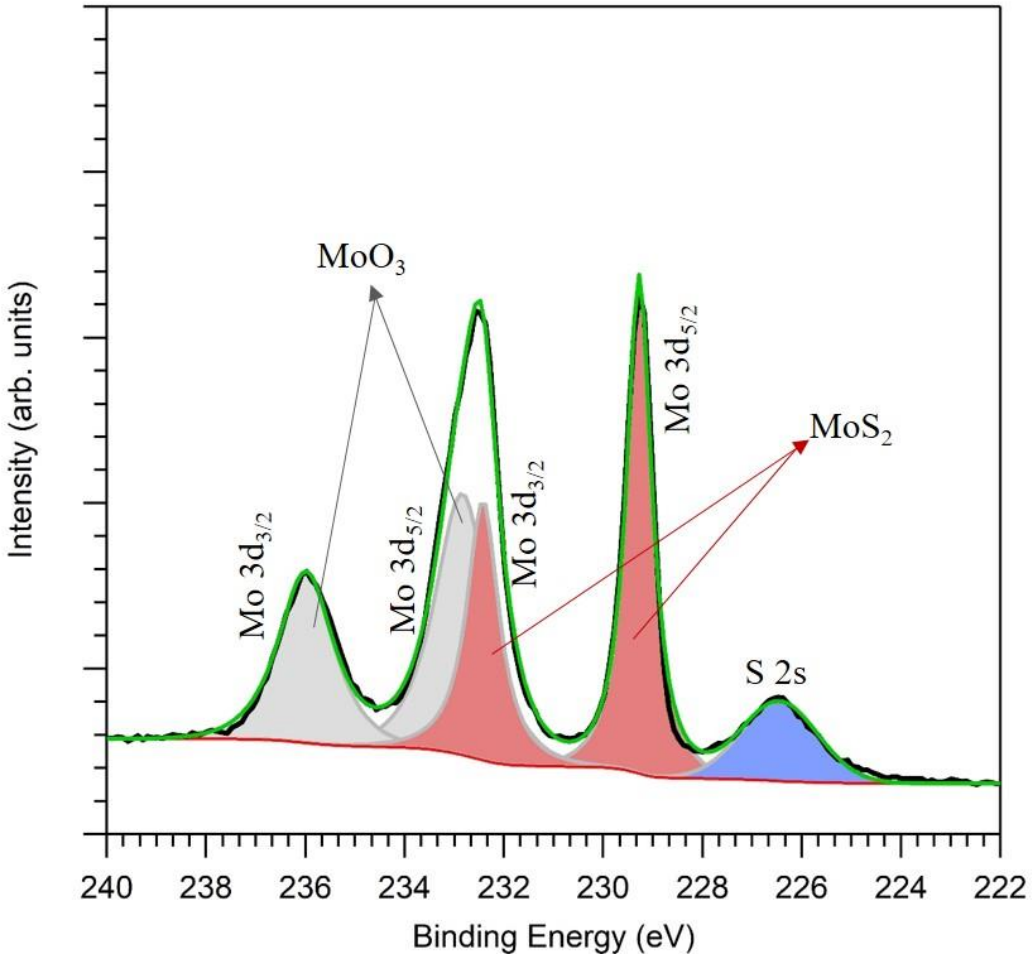

Figure 31. Mo 3d and S 2s core levels of a molybdenum thin film partially oxidized and partially sulfurized. Raw data is in black, envelop is in green, Mo $3d_{5/2}$ and Mo $3d_{3/2}$ ascribed to MoS_2 are in light red while the respective Mo 3d components ascribed to MoO_3 are in grey and S 2s is in blue.

The procedure for fitting this spectra consists of a series of step. First, a Shirley background is drawn from the edges of the spectrum. Then, there are some clues that facilitate the analysis. For example, if S 2p was detected in the wide scan, it is expected to have also the S 2s peak in this region; it is the peak at lower BE in the spectrum. It is also known that Mo 3d spectrum shows the spit orbit splitting couple, Mo $3d_{5/2}$ and Mo $3d_{3/2}$. This way, S 2s, Mo $3d_{5/2}$ from MoS_2 and Mo $3d_{3/2}$ from MoO_3 appear as single peaks in the spectra of figure 32 and thus, they can be fitted as single components. The complex part of the fitting is at the centre of the Mo 3d core level. Near 233 eV Mo $3d_{3/2}$ from MoS_2 overlap with Mo $3d_{5/2}$ from MoO_3. For fitting this region of the spectra we can take advantage of the known relations between the different components. On one hand, the spin-orbit splitting, *i.e.* the difference in energy between Mo $3d_{5/2}$ and Mo $3d_{3/2}$ is of about 3.15 eV. On the other hand, the ratio between the areas of Mo $3d_{3/2}$ and Mo $3d_{5/2}$ is around 2:3. This way, by including this two constrains in the fitting routine, the whole spectra can be fitted [4].

Furthermore, after fitting it is possible to know the ratio between MoO_3 and MoS_2 at the surface of the sample by using equation 3. The areas of the two Mo $3d_{5/2}$ core levels are parameters obtained from the fitting, the sensitivity factors or cross sections are the same because of two peaks of the same element are under comparison and finally, the transmission of the system is also the same because the two components appears at almost the same energy. Thus, the ratio between MoO_3 and MoS_2 in this case is the ratio between the areas of the Mo $3d_{5/2}$ peaks obtained from the fitting showed in figure 31.

The overlapping of different components can be deconvoluted by fitting the XPS spectra

Abbreviations

AES: Auger Electron Spectroscopy

ARXPS: Angle Resolved X-ray Photoelectron Spectroscopy

BE: Binding Energy

CB: Conduction Band

CVD: Chemical Vapour Deposition

ESCA: Electron Spectroscopy for Chemical Analysis

eV: Electron volts

FAT: Fixed Analyser Transmission

FE: Fermi Edge

FWHM: Full Width at Half Maximum

hν: Photon Energy

KE: Kinetic Energy

PS: Photoelectron spectroscopy

TSP: Titanium Sublimation Pump

UHV: Ultra High Vacuum

UPS: Ultra-Violet Photoelectron Spectroscopy

VB: Valence Band

XPS: X-ray Photoelectron Spectroscopy

ϕ: Work Function

ϕ_s: Work Function of the spectrometer

References

[1] J. Azpeitia, G. Otero-Irurueta, I. Palacio, J.I. Martinez, N. Ruiz del Árbol, G. Santoro, A. Gutiérrez, L. Aballe, M. Foerster, M. Kalbac, V. Vales, F.J. Mompeán, M. García-Hernández, J.A. Martín-Gago, C. Munuera and M.F. López. *"High-quality PVD graphene growth by fullerene decomposition on Cu foils". Carbon* **119** (2017) 535–543

[2] I. Bdikin, D.K. Sharma, G. Otero-Irurueta, M.J. Hortigüela, P.K. Tyagi, V. Neto and M.K. Singh. *"Charge injection in large area multilayer graphene by ambient Kelvin probe force microscopy". Appl. Mater. Today.* **8** (2017) 18–25

[3] I. Palacio, G. Otero-Irurueta, C. Alonso, J.I. Martínez, E. López-Elvira, I. Muñoz-Ochando, H.J. Salavagione, M.F. López, M. García-Hernández, J. Méndez, G.J. Ellis and J.A. Martín-Gago. *"Chemistry below graphene: Decoupling epitaxial graphene from metals by potential-controlled electrochemical oxidation". Carbon* **129** (2018) 837–846

[4] D.K. Sharma, E.V. Ramana, S. Fateixa, M.J. Hortigüela, G. Otero-Irurueta, H.I.S. Nogueira and A. Kholkin. *"Pressure-dependent large area synthesis and electronic structure of MoS2". Mater. Res. Bull.* **97** (2018) 265–271.

[5] B. Brox and I. Olefjord. *"ESCA Studies of MoO2 and MoO3". Surf. Interface Anal.* **13** (1988) 3–6

[6] Y. Lee, J. Lee, H. Bark, I.-K. Oh, G.H. Ryu, Z. Lee, H. Kim, J.H. Cho, J.-H. Ahn and C. Lee. *"Synthesis of wafer-scale uniform molybdenum disulfide films with control over the layer number using a gas phase sulfur precursor". Nanoscale* **6** (2014) 2821

[7] A.F. Girão, G. Gonçalves, K.S. Bhangra, J.B. Phillips, J. Knowles, G. Irurueta, M.K. Singh, I. Bdkin, A. Completo and P.A.A.P. Marques. *"Electrostatic self-assembled graphene oxide-collagen scaffolds towards a three-dimensional microenvironment for biomimetic applications". RSC Adv.* **6** (2016) 49039–49051

[8] G. Otero-Irurueta, J.I. Martínez, R.A. Bueno, F.J. Palomares, H.J. Salavagione, M.K. Singh, J. Méndez, G.J. Ellis, M.F. López and J.A. Martín-Gago. *"Adsorption and coupling of 4-aminophenol on Pt(111) surfaces". Surf. Sci.* **646** (2016) 5–12

[9] D. Usachov, O. Vilkov, A. Grüneis, D. Haberer, A. Fedorov, V.K. Adamchuk, A.B. Preobrajenski, P. Dudin, A. Barinov, M. Oehzelt, C. Laubschat and D.V. Vyalikh. *"Nitrogen-Doped Graphene: Efficient Growth, Structure, and Electronic Properties". Nano Lett.* **11** (2011) 5401–5407

[10] D.M. Tobaldi, R.C. Pullar, A.F. Gualtieri, G. Otero-Irurueta, M.K. Singh, M.P. Seabra and J.A. Labrincha. *"Nitrogen-modified nano-titania: True phase composition, microstructure and visible-light induced photocatalytic NOx abatement". J. Solid State Chem.* **231** (2015) 87–100

[11] D.M. Tobaldi, M.P. Seabra, G. Otero-Irurueta, Y.R. de Miguel, R.J. Ball, M.K. Singh, R.C. Pullar and J.A. Labrincha. *"Quantitative XRD characterisation and gas-phase photocatalytic activity testing for visible-light (indoor applications) of KRONOClean 7000®". RSC Adv.* **5** (2015) 102911–102918